Thermo-Calc Software

TC-Prisma Online Training Course

Day 2 - April 16, 2025

Åke Jansson, Carl Magnus Lancelot, Kevin Wu, Qing Chen

www.thermocalc.com

Schedule

Day 2: TC-PRISMA (Precipitation Module)

09:00	Yesterday's home assignment
09:10	Theoretical Background: Growth Models
09:40	Examples: Ni alloys
10:30	Q & A
10:45	Examples: Steel
11:20	Example: Steel, Para-equilibrium models
11:50	Q & A

Home assignment: Al - Zr Alloy

System	
Database package	ALDEMO + MALDEMO (or TCAL9+MOBAL8)
Elements	Al, Zr, Si, (Fe is optional if TCAL9 used)
Matrix phase	FCC_A1
Precipitate phase	Al_3Sc (= AL3X in TCAL9)
Conditions	
Composition	Al - 0.23 Zr – 0.05 Si (- 0.1 Fe) (wt.%)
Temperature	650 K
Simulation time	500 hours
Nucleation properties	Nucleation Site Type: Bulk

Data Parameters	
Interfacial Energy	Calculated
Molar Volume (Matrix):	Fcc_A1: from database
Molar Volume (Precipitate):	Al_3Sc: from database

Home assignment: Al - Zr Alloy

The aim of this assignment is not only to simulate the precipitation treatment of this alloy, but to compare its simulated hardness (HV) with experimental data from the paper.

Following the paper, it is not the most stable Al-Zr phase that forms during the first several hundred hours of heat treatment. The most stable phase is called AL3ZR_D023 in TCAL and will probably become stable after even longer time at high T. Instead another phase of the same chemistry, AL3X, precipitates first (this phase is called AL3SC in ALDEMO).

The calculation of hardness in TC-Prisma is based on the same principle as the calculation of Yield strength. The selection and setting of parameters is done in the Plot renderer, see next slide.

Use the experimental file ”Souza_data.exp” for comparison with your result.

Precipitation hardening in dilute Al–Zr alloys

Pedro Henrique Lamarão Souza[a,*], *Carlos Augusto Silva de Oliveira*[a], *José Maria do Vale Quaresma*[b]

Home assignment: Al - Zr Alloy

1. In the Plot renderer, select Yield Strength as Y-axis variable.

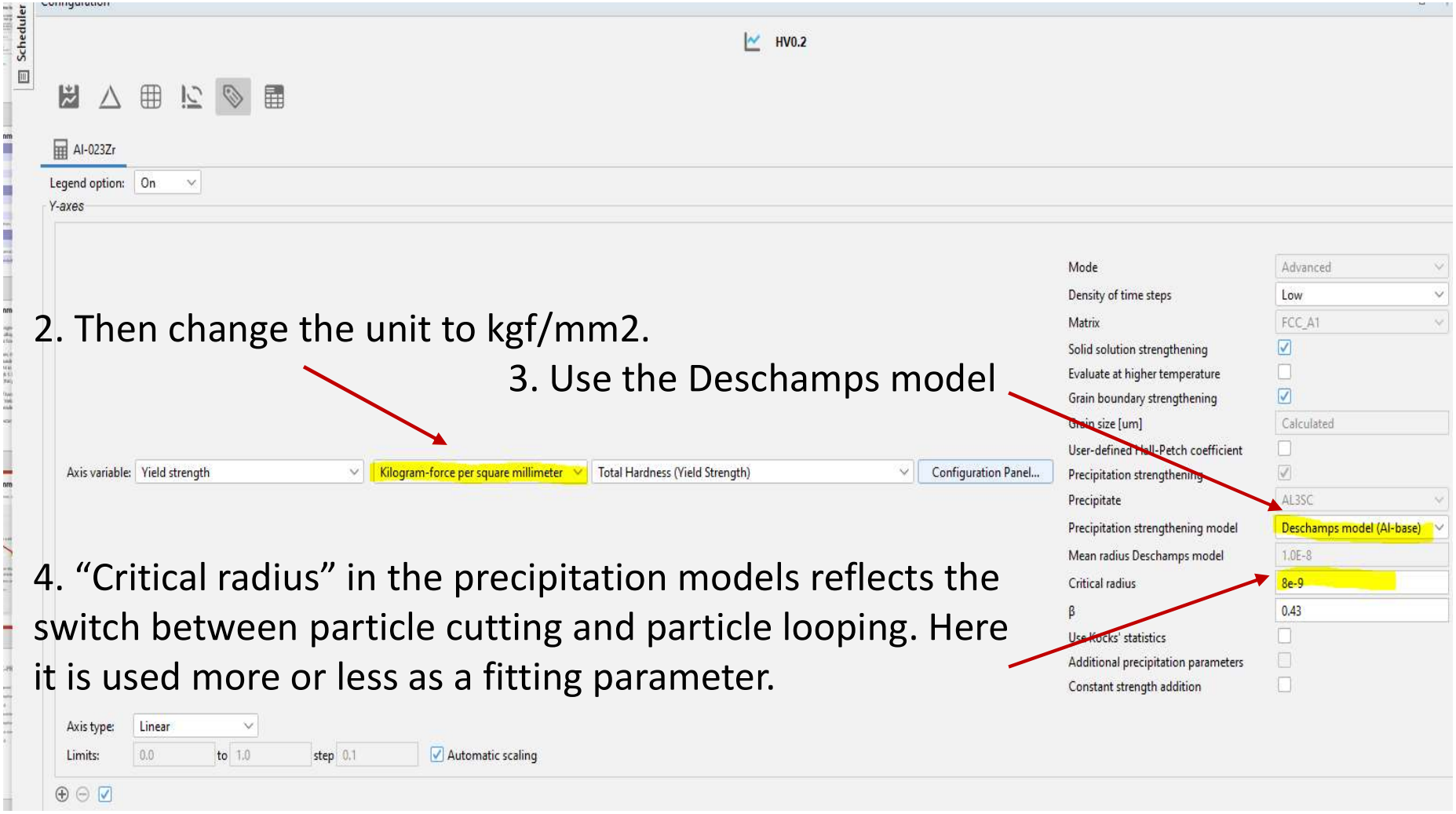

2. Then change the unit to kgf/mm2.

3. Use the Deschamps model

4. “Critical radius” in the precipitation models reflects the switch between particle cutting and particle looping. Here it is used more or less as a fitting parameter.

HA: Al - Zr Alloy - Results

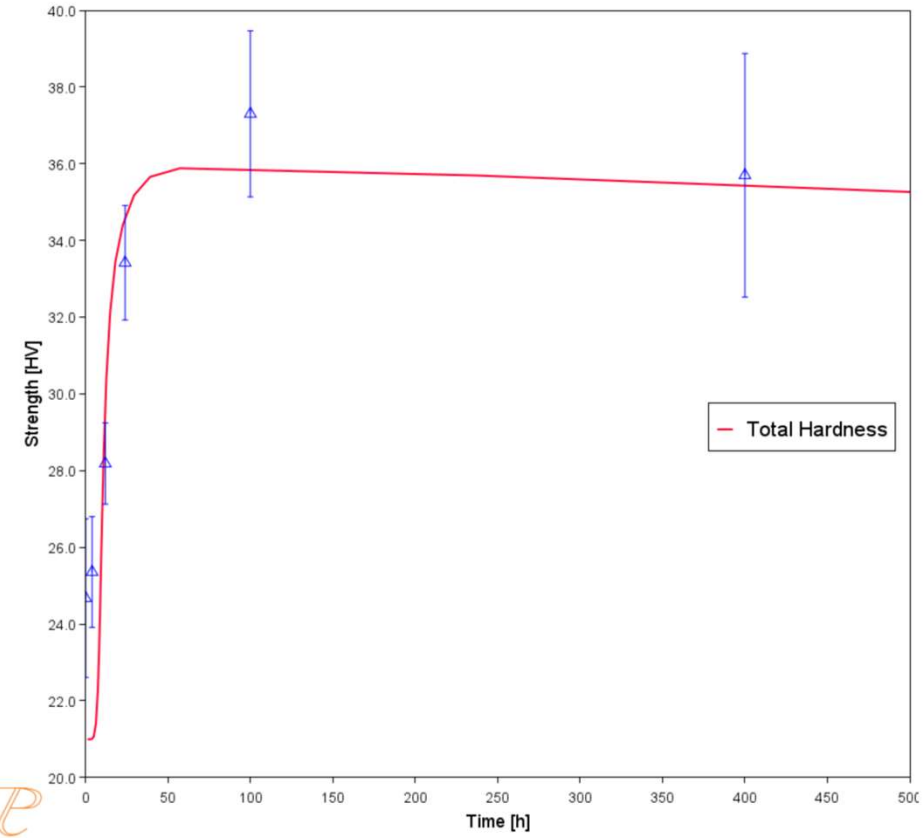

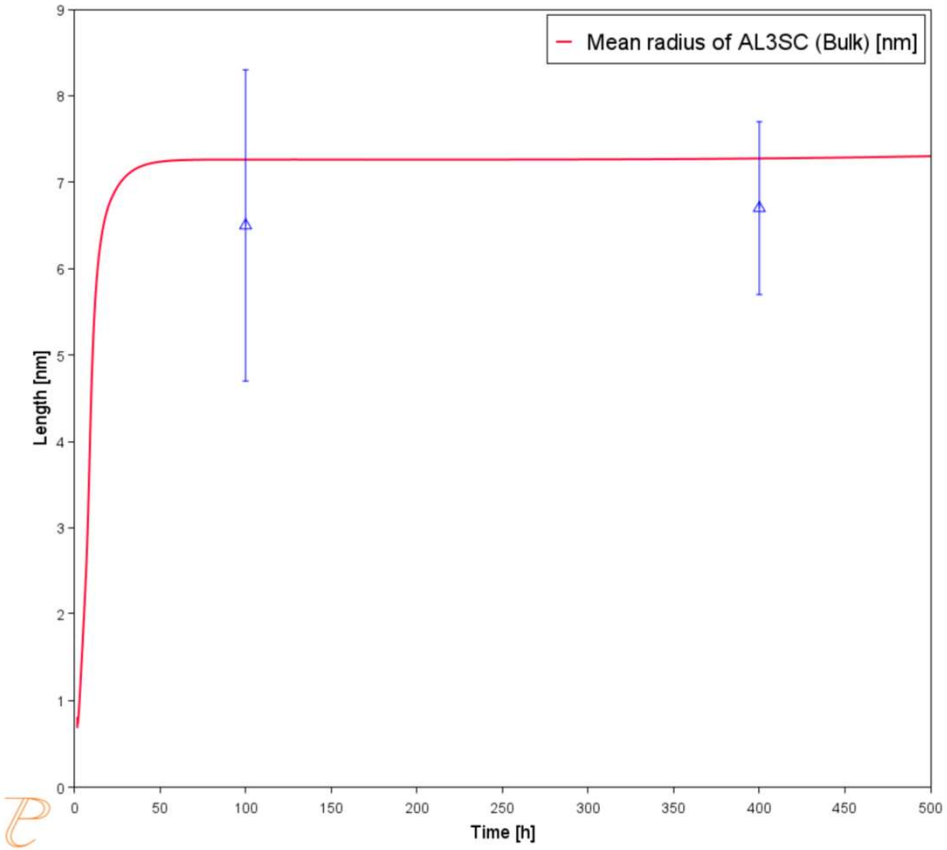

Theory: Growth

Models and Model Parameters

LS (Langer-Schwartz) and KWN (Kampmann and Wagner Numerical) Approach

$$J = \int_{r^*}^{\infty} j(r)dr$$

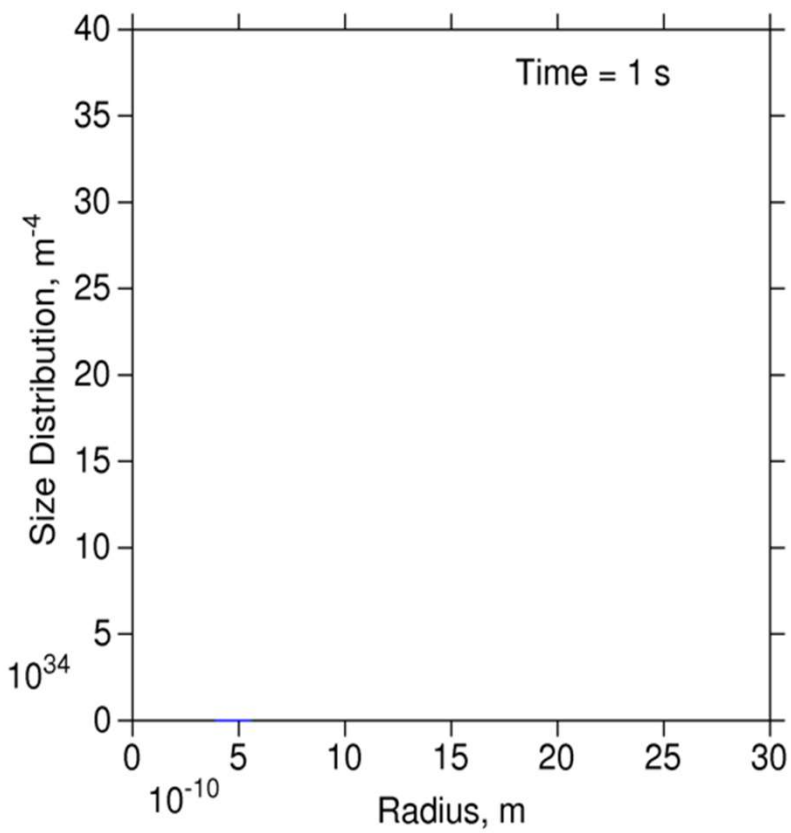

Continuity equation

$$\frac{\partial f(r,t)}{\partial t} = -\frac{\partial}{\partial r}\left[\upsilon(r) f(r,t)\right] + j(r,t)$$

$$C_0^{\alpha} = C^{\alpha} + \left(C^{\beta} - C^{\alpha}\right)\int_0^{\infty} \frac{4\pi}{3} f(r,t) r^3 dr$$

Mass balance

Models: Growth Rate

Available models

- Binary

$$\upsilon = \frac{c^{\alpha} - c^{\alpha/\beta}(r)}{c^{\beta} - c^{\alpha/\beta}(r)} \frac{D}{r}$$

H.B. Aaron, D. Fainstain, G. R. Kotler, J. Appl. Phys., 41(1970)4404

- Multi-Component Coarsening

$$\upsilon = \frac{2\sigma V_m^{\alpha}}{\left(\Delta C^{\alpha\beta}\right]\left[M\right]^{-1}\left[\Delta C^{\alpha\beta}\right)} \frac{1}{r}\left(\frac{1}{r^*} - \frac{1}{r}\right)$$

J.E. Morral, G.R. Purdy, Scripta Metall. Mater., 30(1994)905-908

- PrecipiCalc Model

$$\upsilon = \left(1 + r\sqrt{4\pi N_v r_a}\right)\frac{\Delta\bar{c}_i G_{ij}^{\alpha} \Delta c_j^{\infty} + \bar{c}_{\delta}^{\beta}\left(\bar{\mu}_{\delta}^{\alpha} - \bar{\mu}_{\delta}^{\beta}\right) - 2V_m^{\beta}\sigma / r}{r\Delta\bar{c}_i G_{ij}^{\alpha} D_{jk}^{-1} B_k + 1/M}$$

H.J. Jou et al. Superalloy 2004, p.877-886

Models: Growth Rate

Available models

- Similarity-Supersaturation

$$\upsilon = \frac{S_1\sqrt{D_1}}{2\sqrt{t}} = \frac{S_2\sqrt{D_2}}{2\sqrt{t}} = \cdots \qquad S_i = f\left(\Omega_i\right)$$

T.Sourmail, Ph. D Thesis, Univ. Cambridge, 2002

- Thermodynamic Extremum Principle

$$\dot{\rho}_k = \frac{F - (2\gamma_k/\rho_k)}{RT\rho_k}\left[\sum_{i=1}^{n}\frac{(c_{ki} - c_{0i})^2}{c_{0i}D_{0i}}\right]^{-1}$$

Svoboda J, Fischer FD, Fratzl P, Kozeschnik E. Mater Sci Eng A, 385(2004)166

Models: Growth Rate

- Local equilibrium at interface
- Flux balance equation

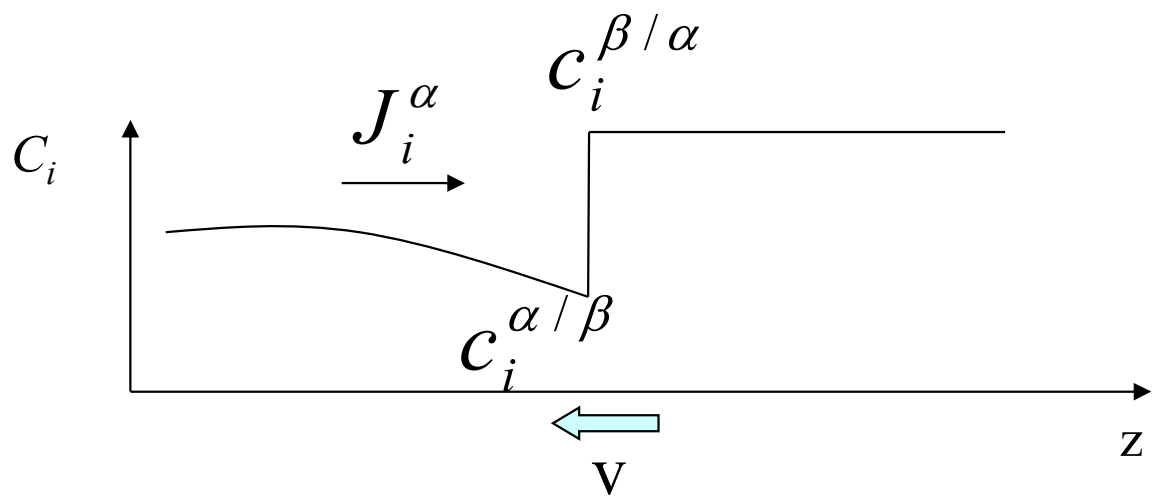

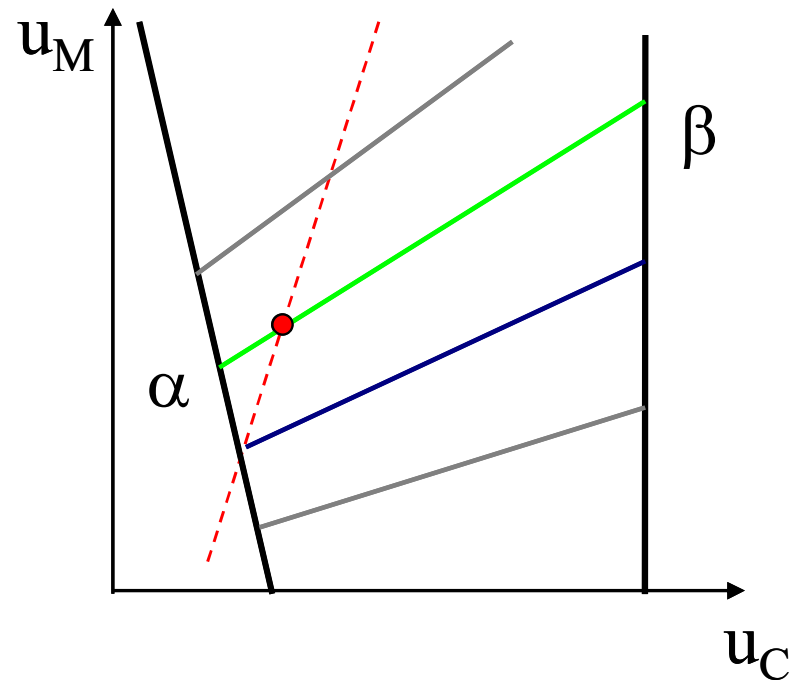

$$\mu_i^{\alpha/\beta} = \mu_i^{\beta/\alpha}$$

$$v(c_i^{\beta/\alpha} - c_i^{\alpha/\beta}) = -J_i^{\alpha} = \sum_j D_{ij}^{\alpha} \frac{\partial c_j^{\alpha}}{\partial z}$$

Models: Growth Rate

Q. Chen, J. Jeppsson, J. Ågren, Acta Mater. 56(2008)1890-1896

Advanced – Analytical Flux-balance Approximation

$$\mu_i^{\alpha/\beta} = \mu_i^{\beta/\alpha} + \frac{2\sigma V_m^{\beta}}{r}$$

$$\upsilon\left(c_i^{\beta/\alpha} - c_i^{\alpha/\beta}\right) = c_i^{\alpha/\beta} M_i \left(\mu_i^{\alpha} - \mu_i^{\alpha/\beta}\right) / \xi_i r$$

Cross diffusion

High supersaturation

General model – new in TC 2019a

$$\upsilon = \frac{K}{r}\left(\Delta G_m - \frac{2\sigma V_m}{r}\right)$$

Models: Growth Rate

General & Simplified – different expressions for *K*

$$\upsilon = \frac{K}{r}\left(\Delta G_m - \frac{2\sigma V_m}{r}\right)$$

Simplified

Similar atomic mobilities

$$K_{sphere}^{simplified} = \left[\sum_i \frac{\left(X_i^{\beta/\alpha}(r) - X_i^{\alpha/\beta}(r)\right)^2 \xi_i}{X_i^{\alpha/\beta}(r) M_i}\right]^{-1}$$

Number fixed Coarsening

General

Very different atomic mobilities

$$K_{sphere}^{Morral-Purdy} = \left[\left(\Delta X^{\alpha\beta}\right]\left[M\right]^{-1}\left[\Delta X^{\alpha\beta}\right)\right]^{-1}$$

Volume fixed Coarsening

General

Very different atomic mobilities

$$K_{sphere}^{general} = \left[\left(\Delta X^{\alpha\beta}\right]\left[\ddot{G}\right]\left[\bar{D}\right]^{-1}\left[\Delta X^{\alpha\beta}\right)\right]^{-1}$$

Volume fixed Growth

Models: Growth Rate

Para-equilibrium and Non-partitioning local equilibrium

$$\upsilon = \frac{K^{PE/NPLE}}{r}\left(\Delta G_m^{PE/NPLE} - \frac{2\sigma V_m}{r}\right)$$

$$K_{sphere}^{PE/NPLE} = \left[\sum_i \frac{\left(u_C^{\beta/\alpha}(r) - u_C^{\alpha/\beta}(r)\right)^2 \xi_C}{u_C^{\alpha/\beta}(r) M_C}\right]^{-1}$$

$$\beta^* = \frac{4\pi r^{*2} K}{a^4}$$

Models: NPLE and Para-eq.

Models to handle NPLE (non partitioning local equilibrium) and para-equilibrium were introduced several years ago.

These models deal with fast diffusion processes and are additions to the Simplified growth rate model.

These models need only to consider the movement of the fast diffusing specie, usually an interstitial such as C or N.

The new (2023) **PE Automatic** model enables a smooth transition from Paraequilibrium growth rate model to Simplified growth rate model. The rate of transition process is dependent on the relative differences in diffusion between C and substitutional elements, as well as the differences in driving force between PE and Ortho-Equilibrium (i.e. Local Eq.).

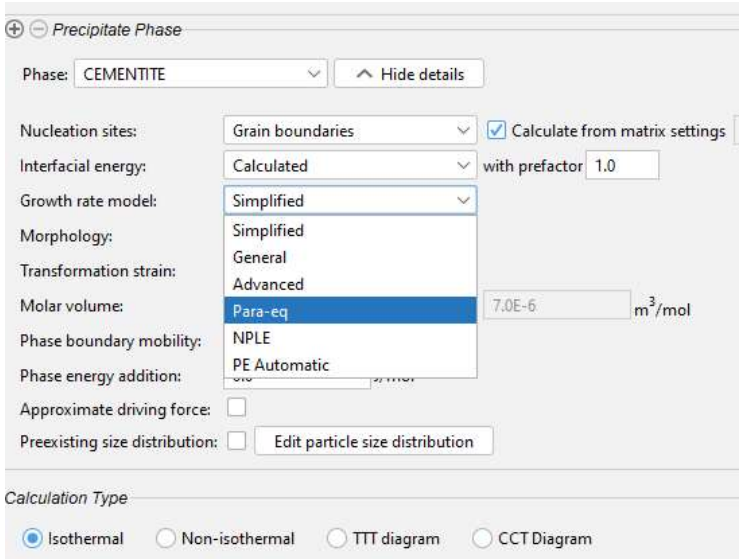

Models: Growth Rate

The non-zero volume correction

$$\upsilon' = \upsilon\left(1 + r\sqrt{4\pi N_V < r >}\right)$$

Chen MK, Voorhees PW, Modeling and simulation in materials science and engineering 1993;1:591-612.

Ortho-eq vs Para-eq

Fe-0.26C-0.11Cr at T= 773 K

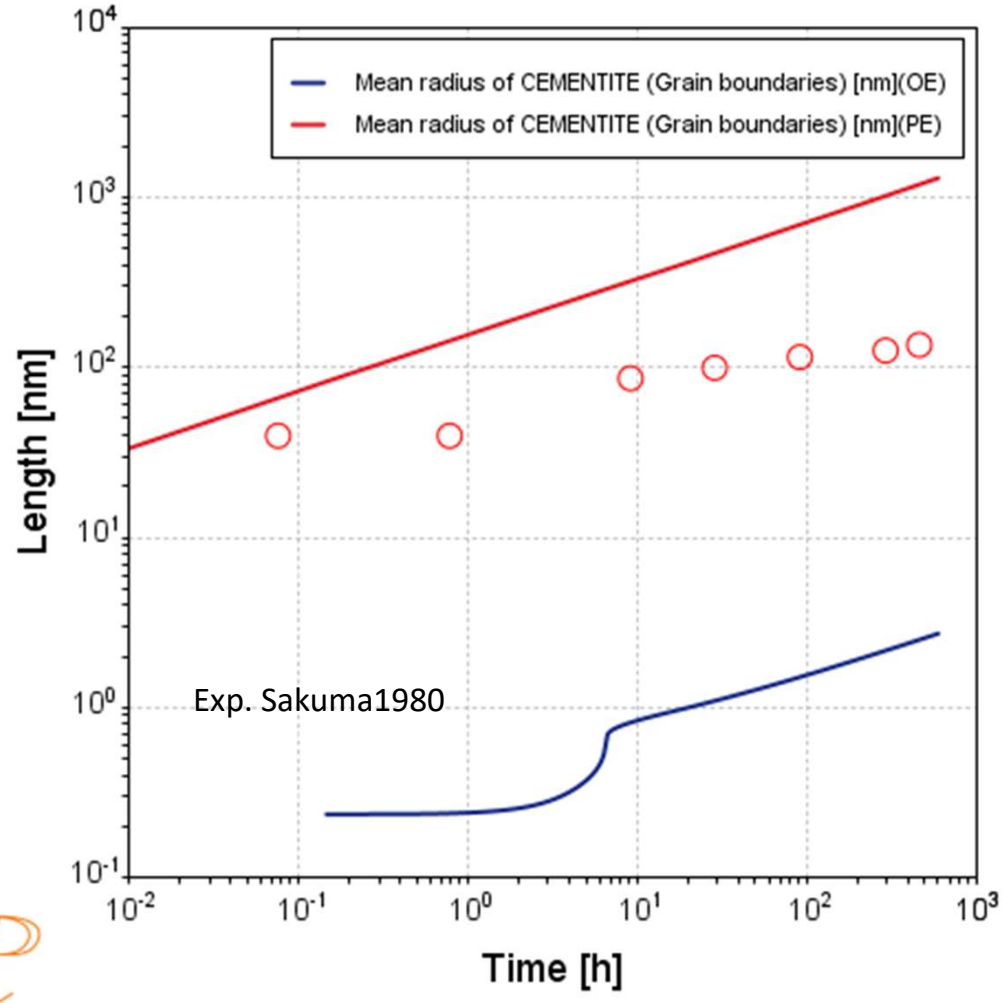

Ortho-eq vs Para-eq

Ultra-high-strength steel at T= 783 K

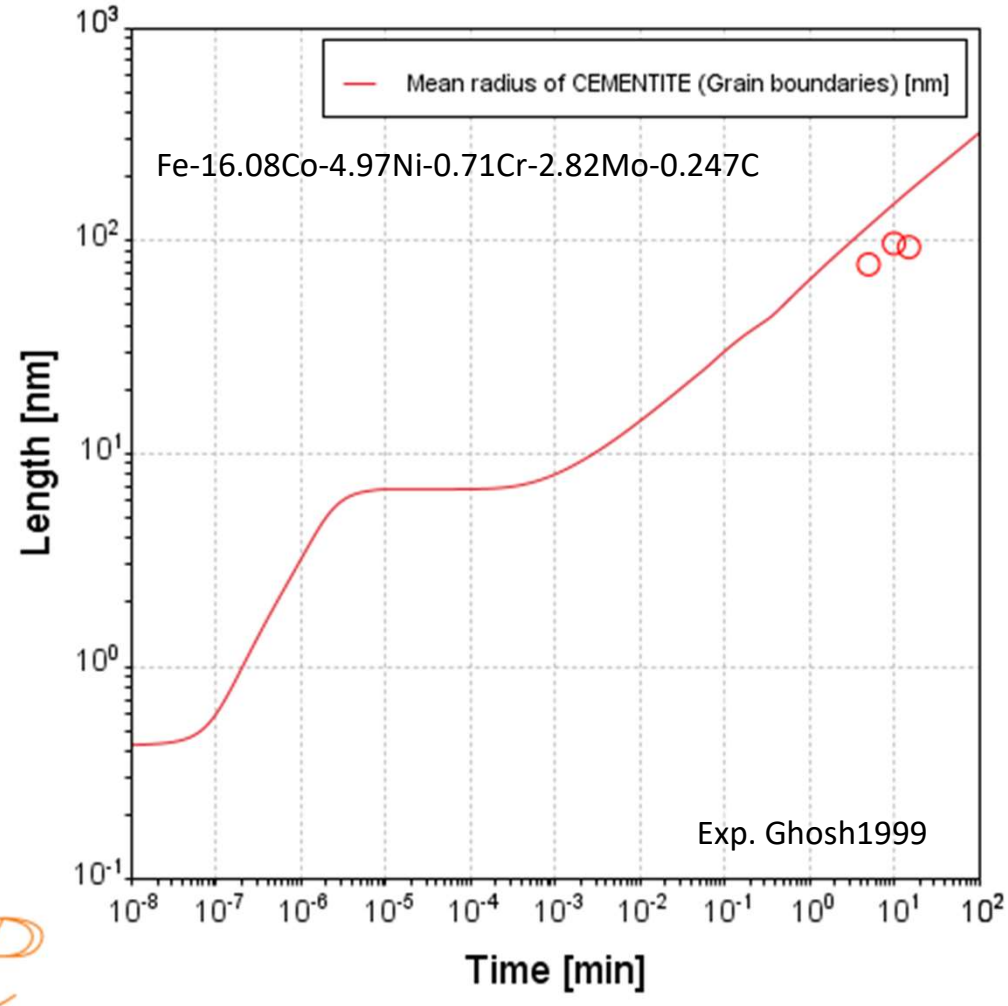

Precipitate Shapes

- **Interfacial Energy Anisotropy***

$$\frac{\sigma_l}{\sigma_r} = \frac{l}{r} = \alpha$$

- **Elastic Strain Energy**
  - Elastically Isotropic or Cubic Systems
  - First Approximation: Elastically Homogenous
  - Eshelby's Theory**

- **Particle Shape**
  - Determined by Minimization of Combined Interfacial Energy and Elastic Energy
  - User-Defined, Fixed Value

Needle
(Prolate Spheroid)

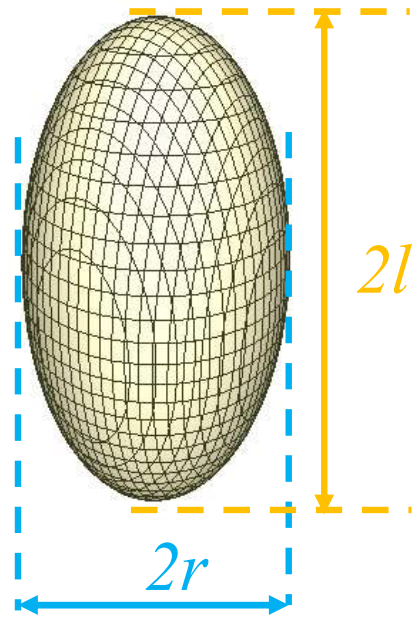

Plate
(Oblate Spheroid)

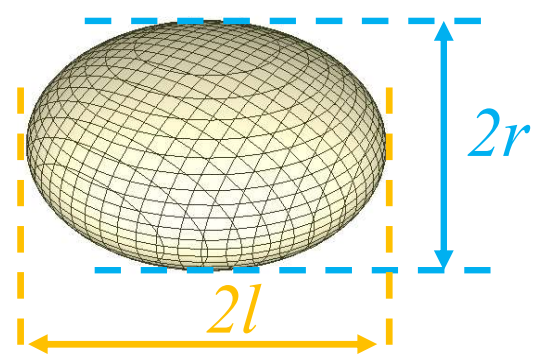

* C.A. Johnson, *Surf. Sci.* 3(1965)429

** J.D. Eshelby, *Pro. Roy. Soc. A*, 241(1957)376

Effect on Growth Rate

K. Wu, Q. Chen, P. Mason, J Phase Eq. Diffus. 39(2018)571-583.

$$\frac{dR}{dt} = K_\sigma \cdot K_{\mathrm{shp}} \cdot \left(\frac{dR}{dt}\right)_{\mathrm{sph}}$$

R: Radius of Equivalent Sphere

- **Interfacial energy anisotropy***
  - Generalized Gibbs-Thomson Effect

$$\mu(R) - \mu(\infty) = K_\sigma \frac{2\sigma_{\mathrm{ch}}^{\mathrm{sp}} V_m}{R}$$

- **Shape Effect**
  - Assumption of Shape Conserving Concentration Field**

Needle* (Prolate Spheroid)**

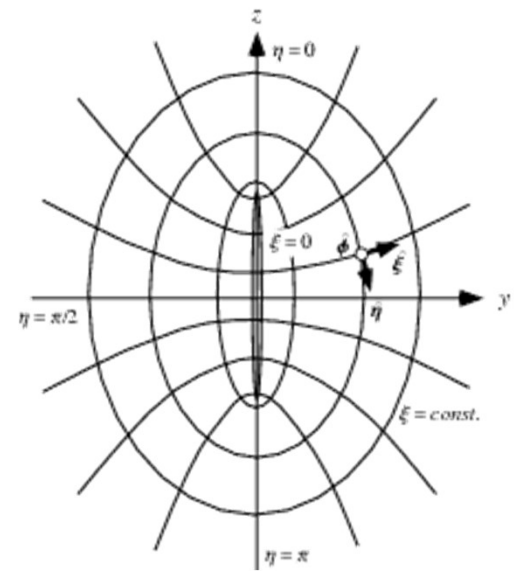

Plate* (Oblate Spheroid)**

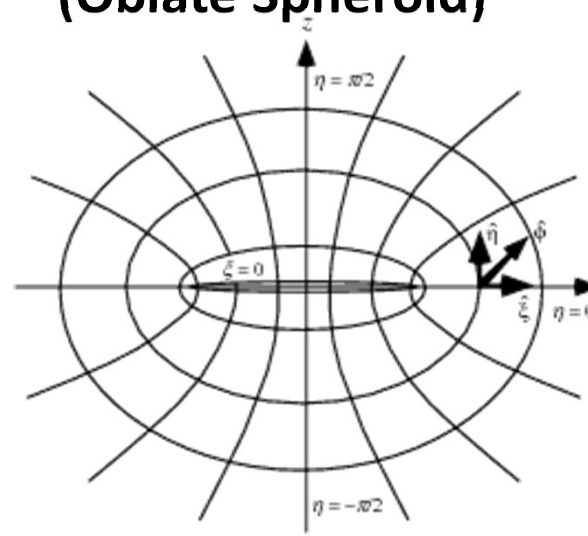

* C.A. Johnson, *Surf. Sci.* 3(1965)429

** F.S. Ham, *Quart. Appl. Math.*, 17(1959)137; *J Phys. Chem. Solids*, 6(1958)335

*** http://http://mathworld.wolfram.com

Effect on Growth Rate

K. Wu, Q. Chen, P. Mason, J Phase Eq. Diffus. 39(2018)571-583.

$$\frac{dR}{dt} = K_\sigma \cdot K_{\text{shp}} \cdot \left(\frac{dR}{dt}\right)_{\text{sph}}$$

R: Radius of Equivalent Sphere

Aspect ratio

$$\alpha = \frac{l}{r} \geq 1$$

Eccentricity

$$e = \sqrt{1 - \frac{1}{\alpha^2}}$$

Needle

$$K_\sigma = \sqrt[3]{\alpha}$$

$$K_{\text{shp}} = \frac{2\sqrt[3]{\alpha^2}e}{\ln(1+e) - \ln(1-e)}$$

α	$K_\sigma K_{shp}$
3.0	1.6
10.0	3.3
15.0	4.4
20.0	5.4

Plate

$$K_\sigma = \sqrt[3]{\alpha^2}$$

$$K_{\text{shp}} = \frac{e\sqrt[3]{\alpha}}{\arccos(0) - \arccos(e)}$$

α	$K_\sigma K_{shp}$
10.0	6.8
15.0	10.0
20.0	13.1

Examples

Ni alloys

TC-PRISMA Example

Available online at www.sciencedirect.com
ScienceDirect
Acta Materialia 56 (2008) 448–463
Acta MATERIALIA
www.elsevier.com/locate/actamat

Effects of a tungsten addition on the morphological evolution, spatial correlations and temporal evolution of a model Ni–Al–Cr superalloy

Chantal K. Sudbrack [a,b], Tiffany D. Ziebell [a,c], Ronald D. Noebe [d], David N. Seidman [a,e,*]

[a] *Department of Materials Science and Engineering, Northwestern University, 2220 Campus Drive, Evanston, IL 60208, USA*
[b] *Materials Science Division, Argonne National Laboratory, Argonne, IL 60439, USA*
[c] *Department of Materials Science and Engineering, Massachusetts Institute of Technology, 77 Massachusetts Avenue, Cambridge, MA 02139, USA*
[d] *NASA Glenn Research Center, 21000 Brookpark Road, Cleveland, OH 44135, USA*
[e] *Northwestern University Center for Atom-Probe Tomography, 2220 Campus Drive, Evanston, IL 60208, USA*

Received 8 July 2007; received in revised form 26 September 2007; accepted 28 September 2007
Available online 26 November 2007

Abstract

The effect of adding 2 at.% W to a model Ni–Al–Cr superalloy on the morphological evolution, spatial correlations and temporal evolution of $\gamma'(L1_2)$-precipitates at 1073 K is studied with scanning electron microscopy and atomic force microscopy. Adding W yields a larger microhardness, earlier onset of spheroidal-to-cuboidal precipitate morphological transition, larger volume fraction (from ~20% to 30%), reduction in coarsening kinetics by one-third and a larger number density (N_v) of smaller mean radii ($\langle R \rangle$) precipitates. The kinetics of $\langle R \rangle$ and interfacial area per unit volume obey $t^{1/3}$ and $t^{-1/3}$ relationships, respectively, which is consistent with coarsening driven by interfacial energy reduction. The N_v power-law dependencies deviate, however, from model predictions, indicating that a stationary state is not achieved. Quantitative analyses with precipitate size distributions, pair correlation functions and edge-to-edge inter-precipitate distance distributions give insight into two-dimensional microstructural evolution, including the elastically driven transition from a uniform γ'-distribution to one-dimensional $\langle 001 \rangle$-strings to eventually clustered packs of γ'-precipitates in the less densely packed Ni–Al–Cr alloy.

Ni-alloy Example 1

System	
Database package	TCNI12 + MOBNI6
Elements	Ni, Al, Cr
Matrix phase	DIS_FCC_A1
Precipitate phases	FCC_L12#2
Conditions	
Composition	Ni – 9.8 Al – 8.3 Cr (at.%)
Temperature	800 °C
Simulation time	1E6 s
Nucleation properties	Nucleation Site Type: Bulk
Data Parameters – Interfacial Energies	
Interfacial Energy	Calculated
Molar Volume (Matrix phase):	DIS_FCC_A1: from database
Molar Volume (Precipitate phase):	FCC_L12#2: from database

Ni-alloy Example 1

Strange result for Volume fraction compared with experimental data from Sudbrack when the setup on previous page is used:

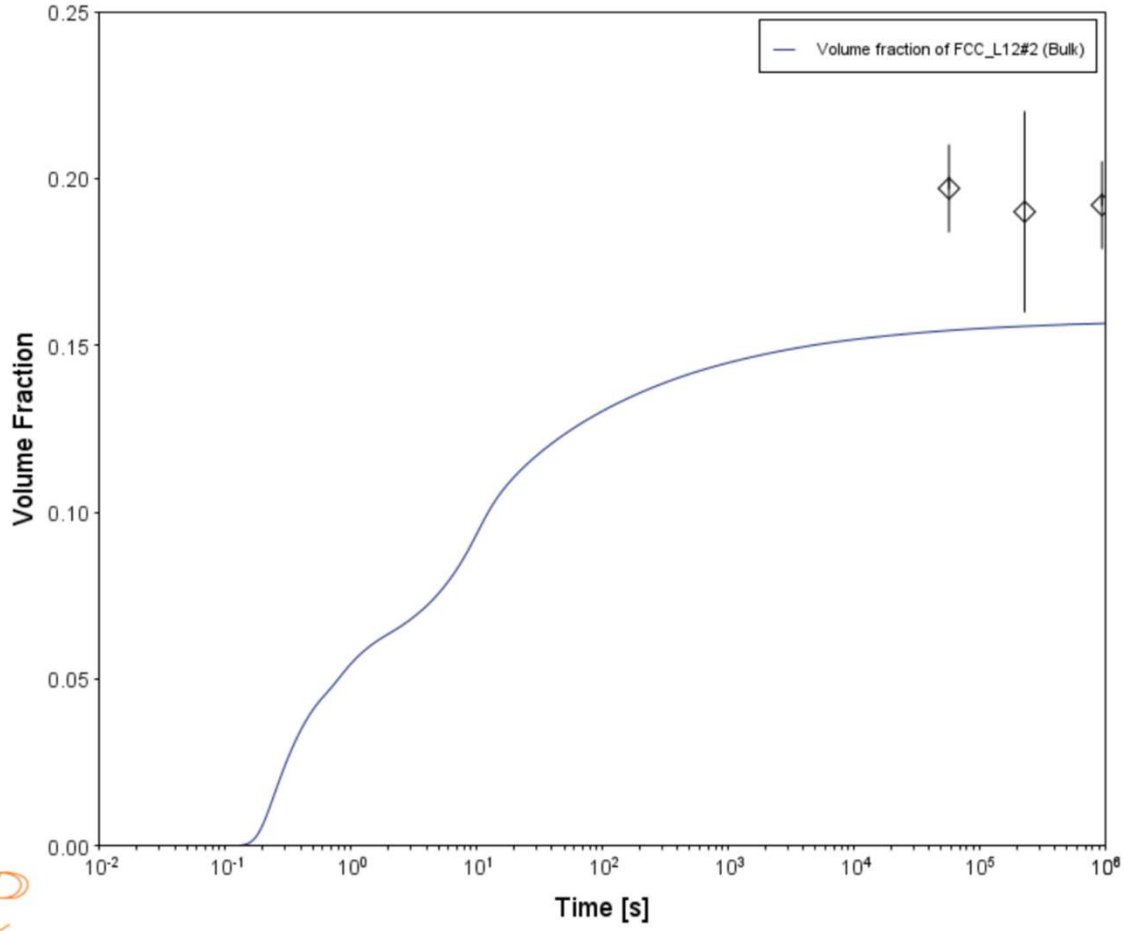

Results

Volume fraction | Number density | Mean radius | Table renderer 1

System

Moles	1.00000	
Mass	55.02701	[g]
Temperature	1073.15000	[K]
Total Gibbs Energy	-66916.16735	[J]
Enthalpy	-51528.57953	[J]
Volume	6.97148E-6	[m³]

Component	*Mole Fraction*	*Mass Fraction*	*Activity*	*Potential*
Al	0.09800	0.04805	8.82663E-10	-1.86021E5
Cr	0.08300	0.07843	0.00136	-58918.48387
Ni	0.81900	0.87352	0.00250	-53474.75936

Stable Phases

	Moles	*Mass*	*Volume Fraction*	
DIS_FCC_A1#1	0.84221	46.67188	0.84210	Composition

Composition

Component	*Mole Fraction*	*Mass Fraction*
Ni	0.82880	0.87777
Cr	0.08612	0.08081
Al	0.08508	0.04142

	Moles	*Mass*	*Volume Fraction*	
FCC_L12#2	0.15779	8.35514	0.15790	Composition

Composition

Component	*Mole Fraction*	*Mass Fraction*
Ni	0.76668	0.84977
Al	0.16698	0.08509
Cr	0.06634	0.06514

In addition, the fit for mean radius as function of time, is not very good.

Ni-alloy Example 1

System	
Database package	TCNI12 + MOBNI6
Elements	Ni, Al, Cr
Matrix phase	DIS_FCC_A1
Precipitate phases	FCC_L12#2
Conditions	
Composition	Ni – 9.8 Al – 8.3 Cr (at.%)
Temperature	800 °C
Simulation time	1E6 s
Nucleation properties	Nucleation Site Type: Bulk
Data Parameters – Interfacial Energies	
Interfacial Energy	Calculated
Molar Volume (Matrix phase):	DIS_FCC_A1: from database
Molar Volume (Precipitate phase):	FCC_L12#2: from database

8.9 Cr

Ni-alloy Example 1

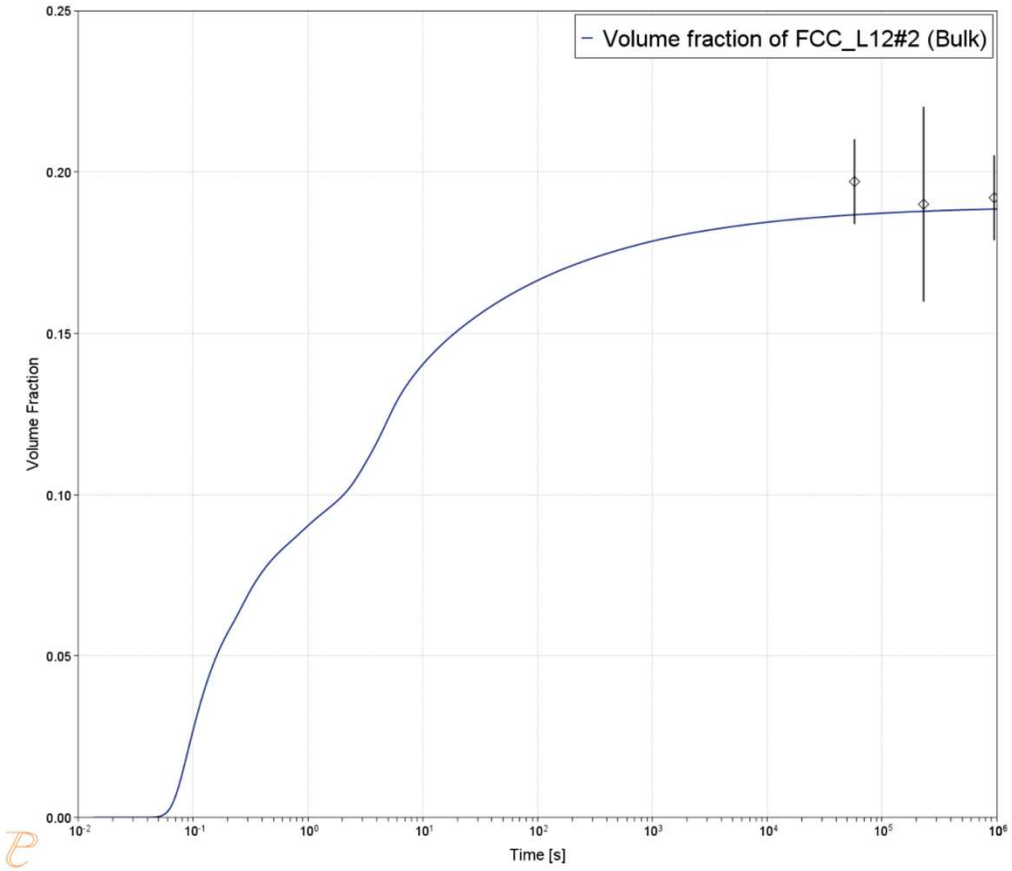

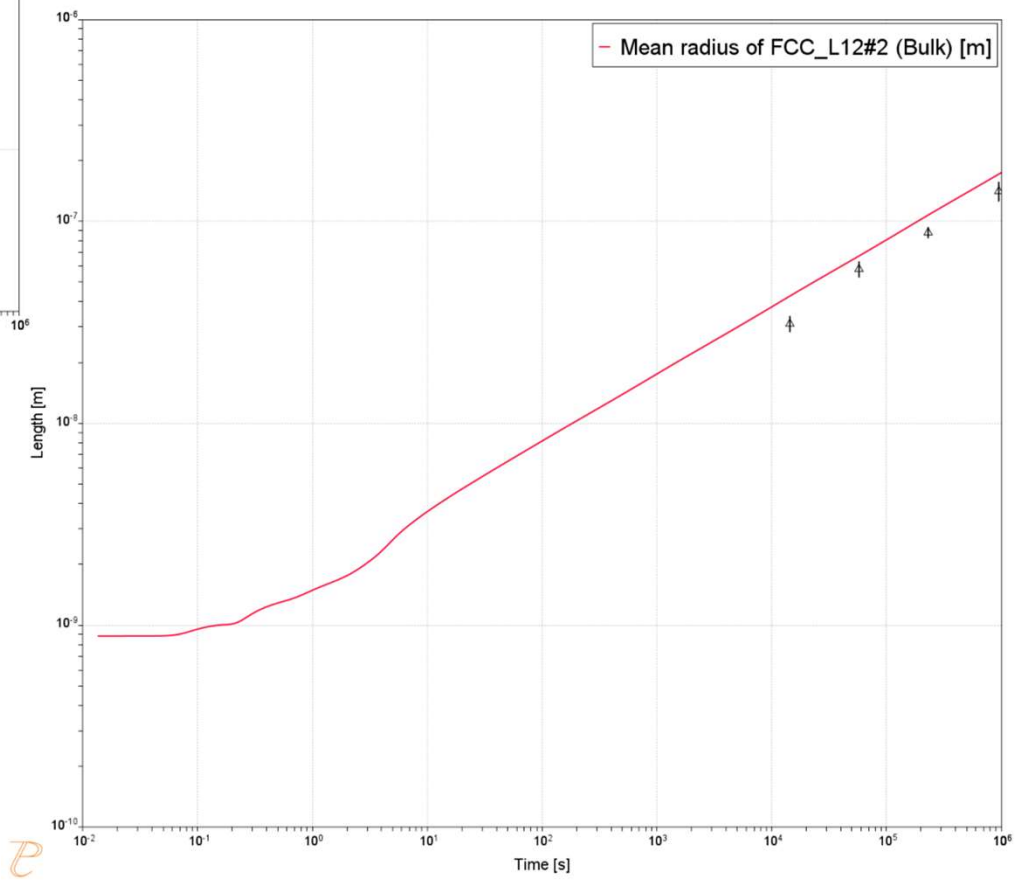

Using Ni – 9.8 Al – 8.9 Cr (at-%)

Ni-8Al-8Cr and Ni-10Al-10Cr

J Mater Sci (2013) 48:825–831
DOI 10.1007/s10853-012-6802-7

Influence of composition on monomodal versus multimodal γ' precipitation in Ni–Al–Cr alloys

T. Rojhirunsakool · S. Meher · J. Y. Hwang · S. Nag · J. Tiley · R. Banerjee

Abstract This study investigates the influence of alloy composition on γ' precipitation in Ni–8Al–8Cr and Ni–10Al–10Cr at.% during continuous cooling from a supersolvus temperature. When subjected to the same cooling rate, Ni–8Al–8Cr develops a monomodal population, whereas Ni–10Al–10Cr develops a multimodal (primarily bimodal) population of γ' precipitates. The bimodal γ' precipitate size distribution in Ni–10Al–10Cr alloy can be attributed to two successive nucleation bursts during continuous cooling while the monomodal γ' size distribution in Ni–8Al–8Cr results from a single nucleation burst followed by a longer time—wider temperature window for nucleation resulting in a larger number density of precipitates. Three-dimensional atom

Ni-alloy Example 2

System	
Database package	NIDEMO + MNIDEMO
Elements	Ni, Al, Cr
Matrix phase	DIS_FCC_A1
Precipitate phases	FCC_L12#2
Conditions	
Composition	Ni – 10 (8) Al – 10 (8) Cr (at.%)
Temperature	940 - 380 °C
Simulation time	2400 s
Nucleation properties	Nucleation Site Type: Bulk
Data Parameters – Interfacial Energies	
Interfacial Energy	Bulk: 0.023 J/m^2
Molar Volume (Matrix phase):	DIS_FCC_A1: from database
Molar Volume (Precipitate phase):	FCC_L12#2: from database
Mobility Adjustment Factor	1 (i.e. no change)

Ni-alloy Example 2

Ni – 8 Al – 8 Cr

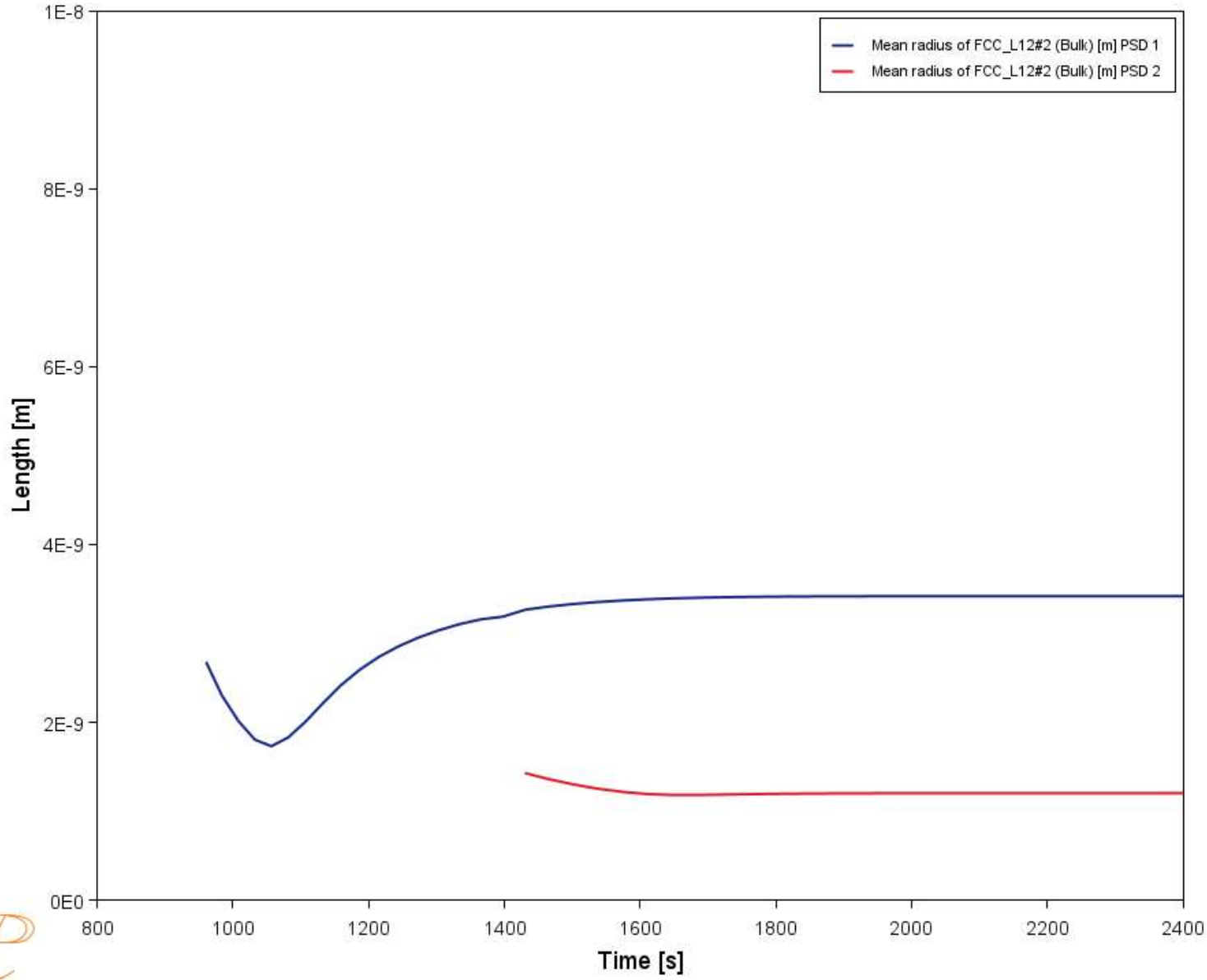

Ni-alloy Example 2

Ni – 10 Al – 10 Cr

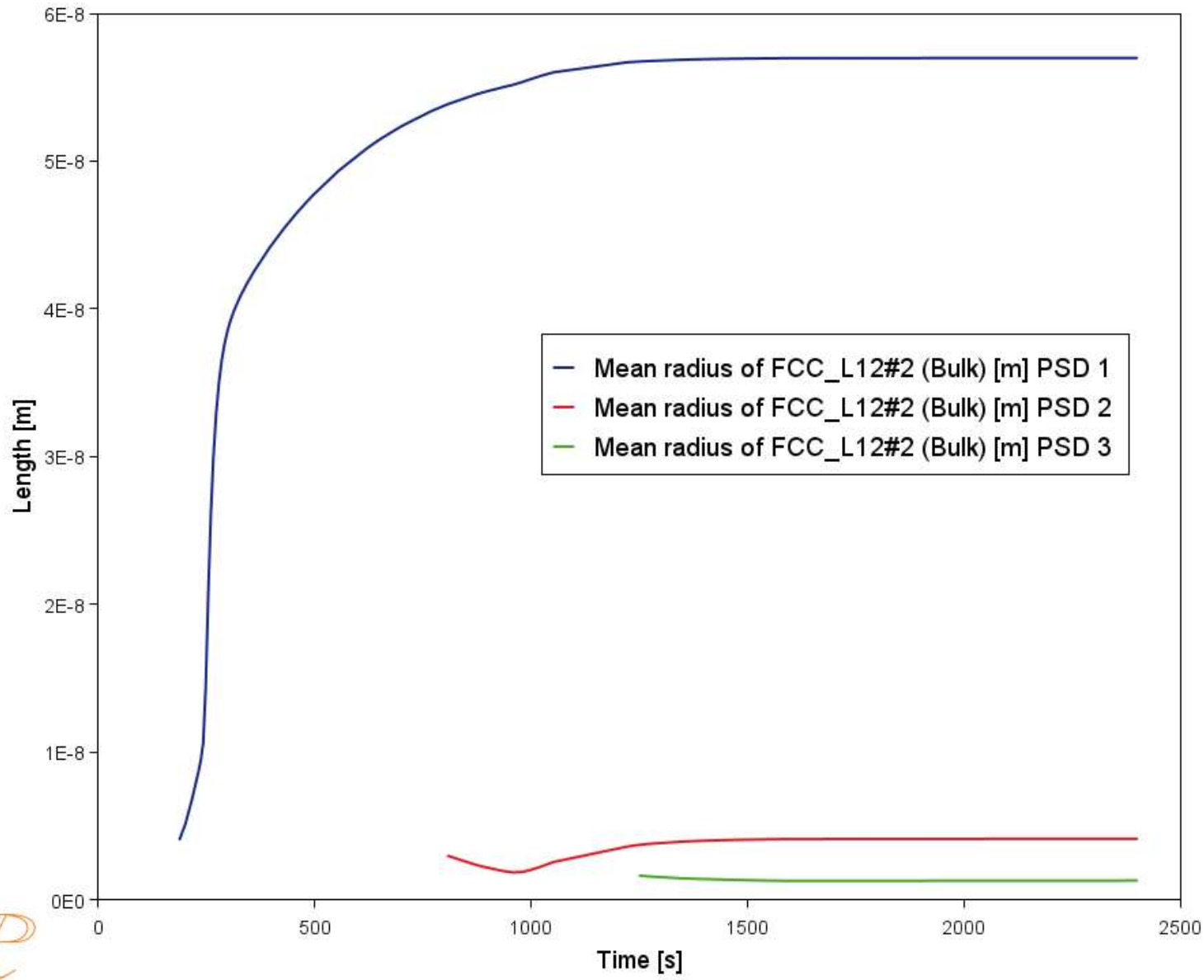

Ni-alloy Example 2

Ni – 8 Al – 8 Cr

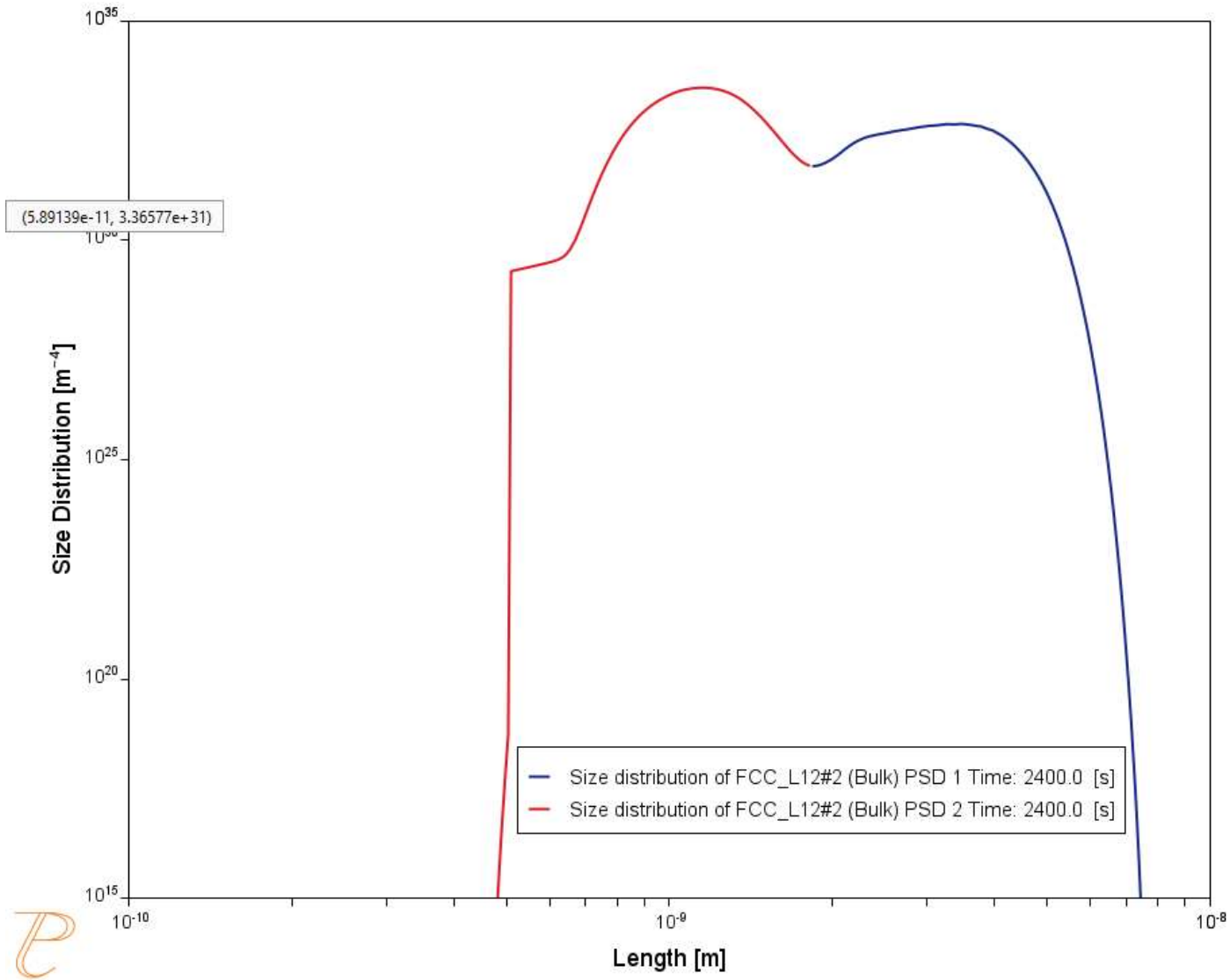

Ni-alloy Example 2

Ni – 10 Al – 10 Cr

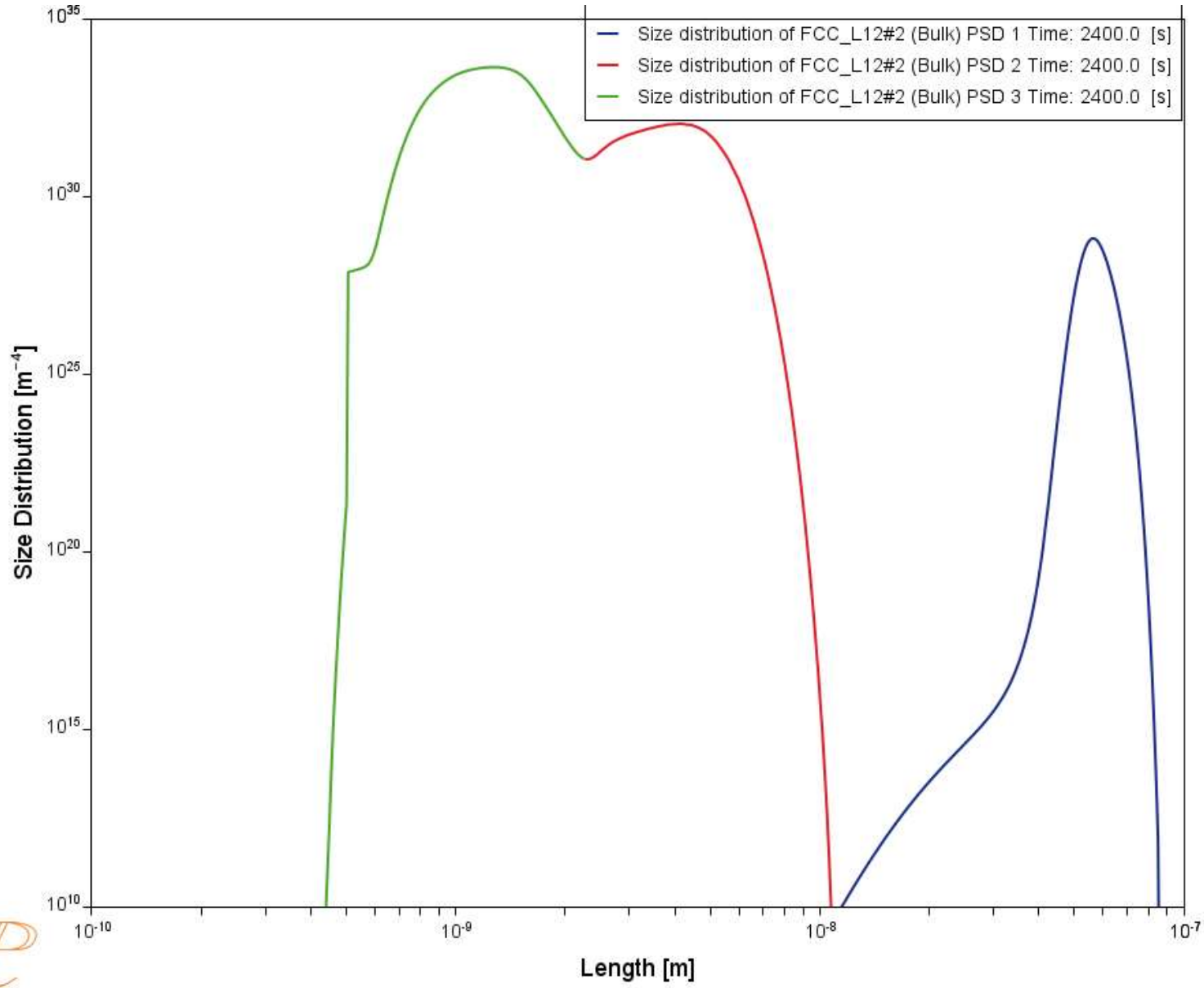

Ni-10Al-10Cr and Ni-8Al-8Cr

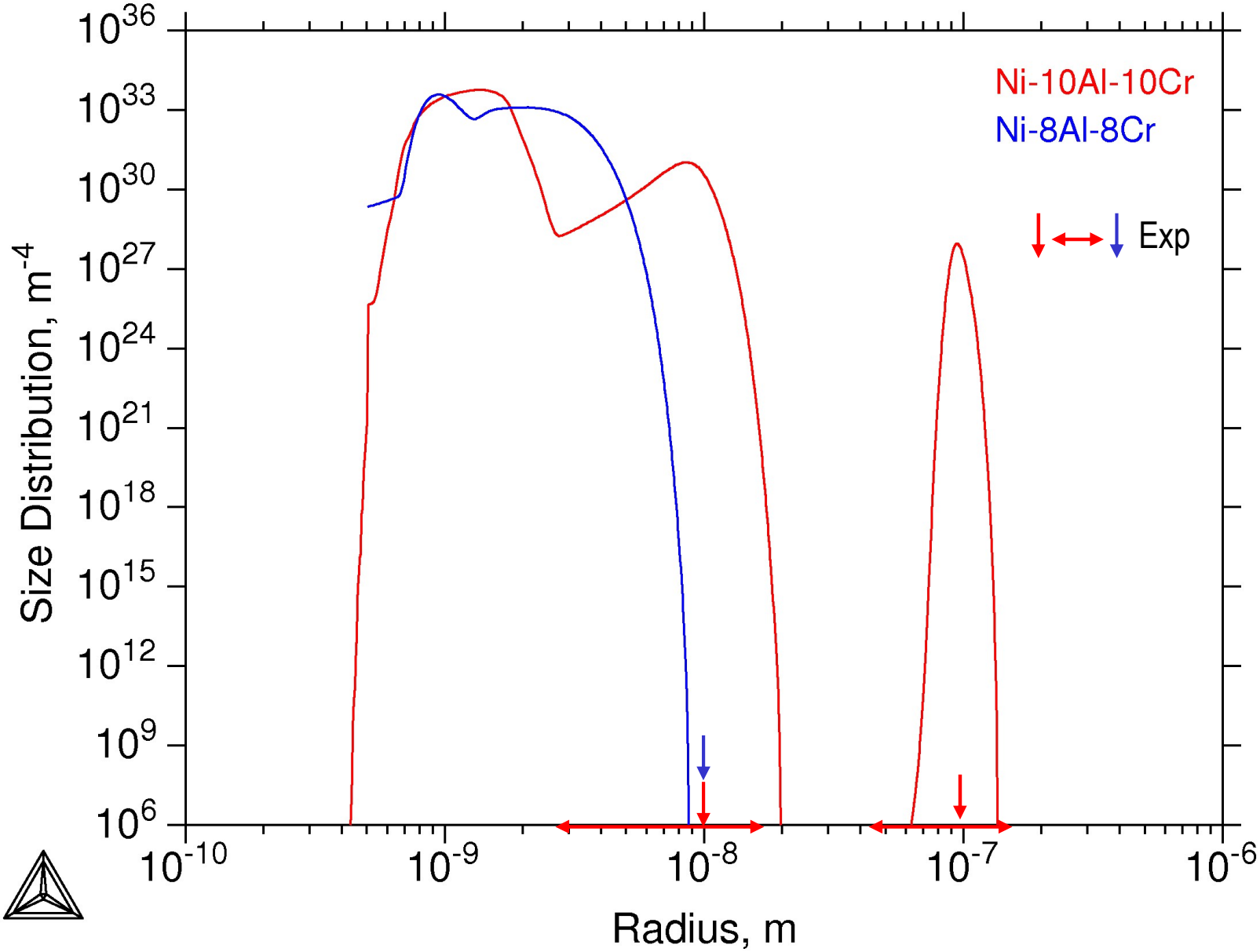

Ni-10Al-10Cr and Ni-8Al-8Cr

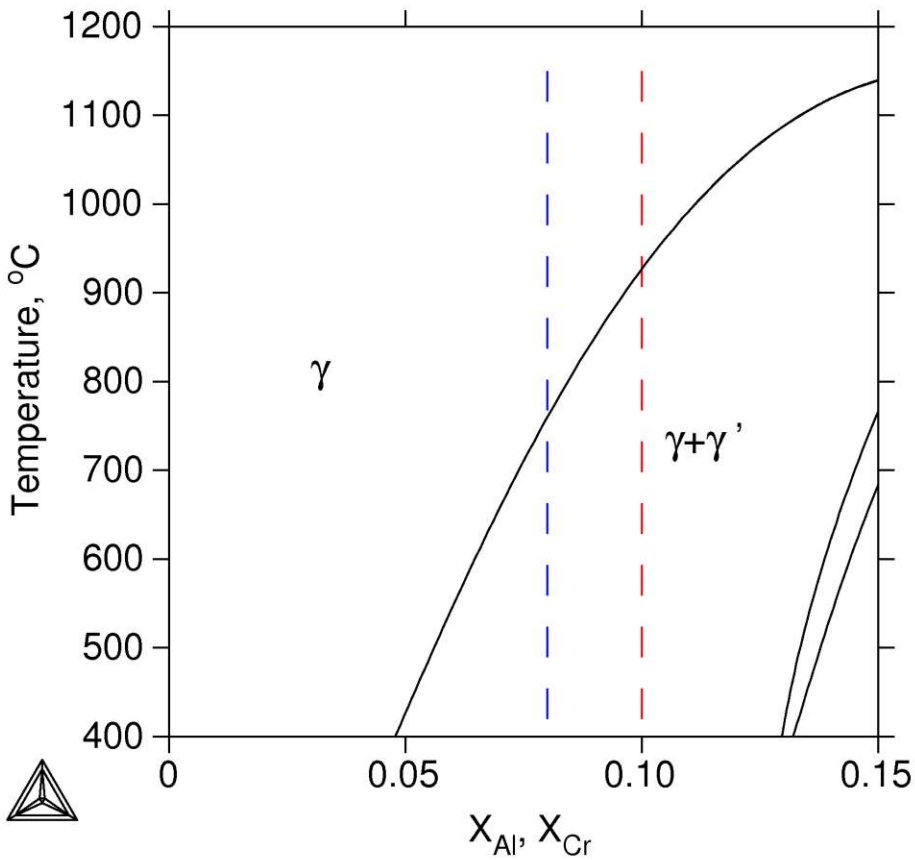

Vertical phase diagram section in Ni-xAl-xCr

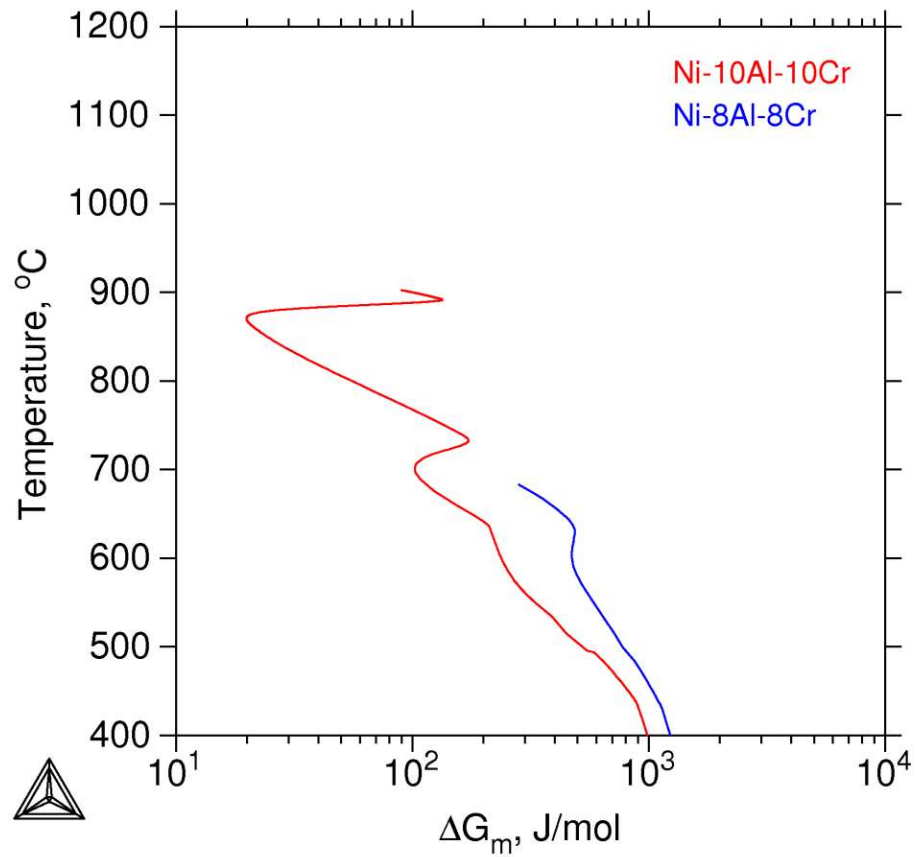

Thermodynamic driving force

Ni-10Al-10Cr and Ni-8Al-8Cr

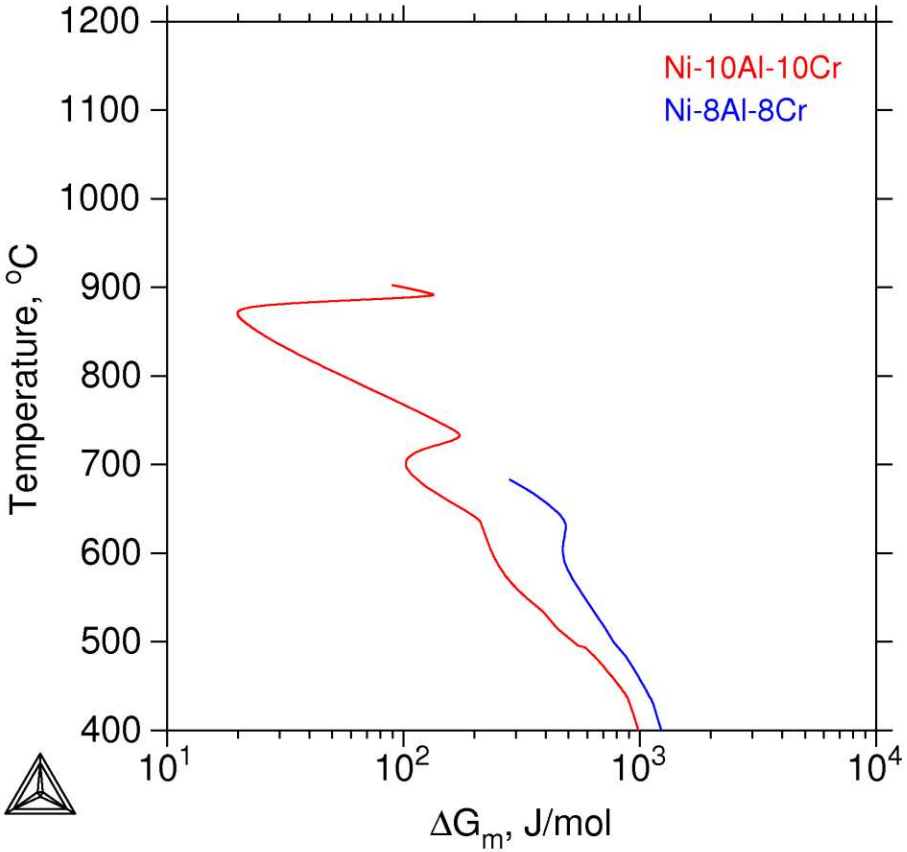

Thermodynamic driving force

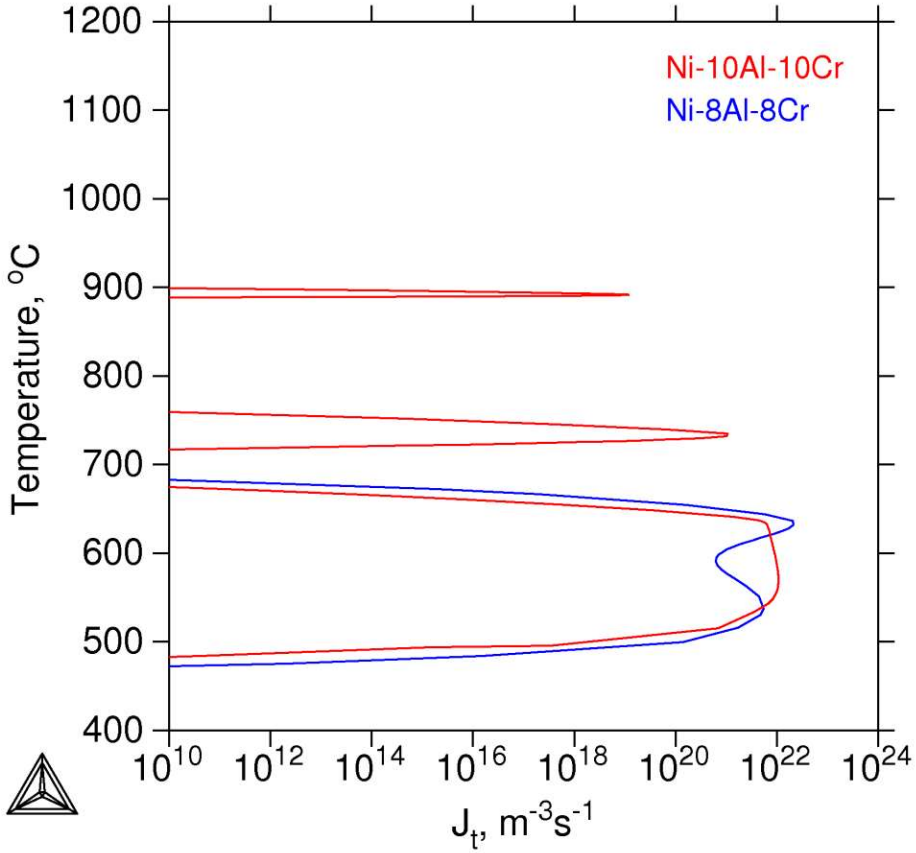

Nucleation rate

U720Li

Precipitation Kinetics during Continuous Cooling

wt.%	1*	2**
Al	2.53	2.46
B	0.014	
C	0.014	0.025
Co	14.43	14.75
Cr	15.92	16.35
Fe	0.09	0.06
Mo	2.96	3.02
Ti	4.96	4.99
W	1.26	1.3
Zr		0.035
Ni	Bal	Bal

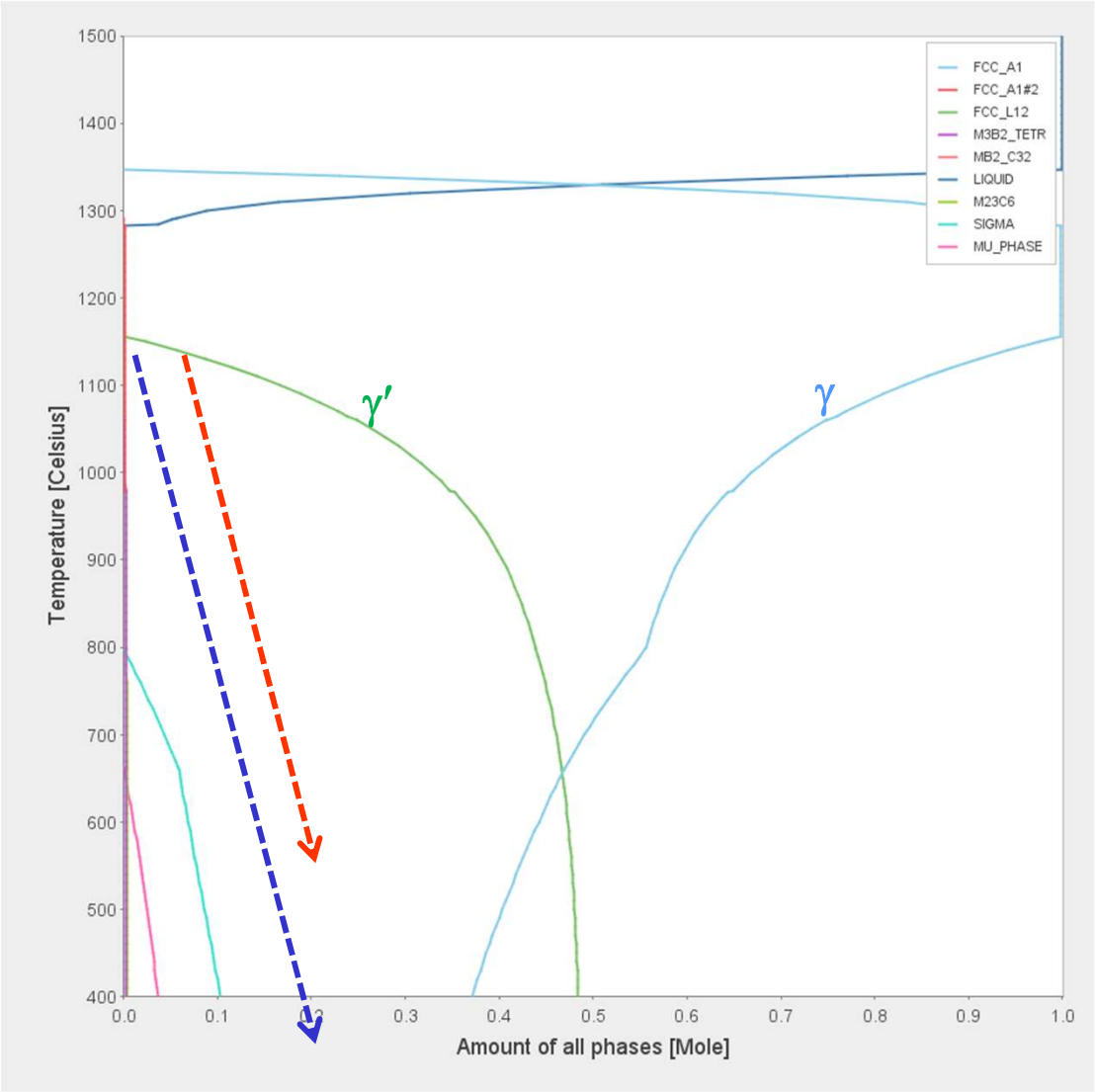

- Databases: TTNI8+MOBNI1

* Radis et al., *Superalloys* 2008 ** Mao et al., *Metall. Mater. Trans. A, 32A(10) 2441(2001)*

U720Li : Cooling Rate Effect

Size Distribution

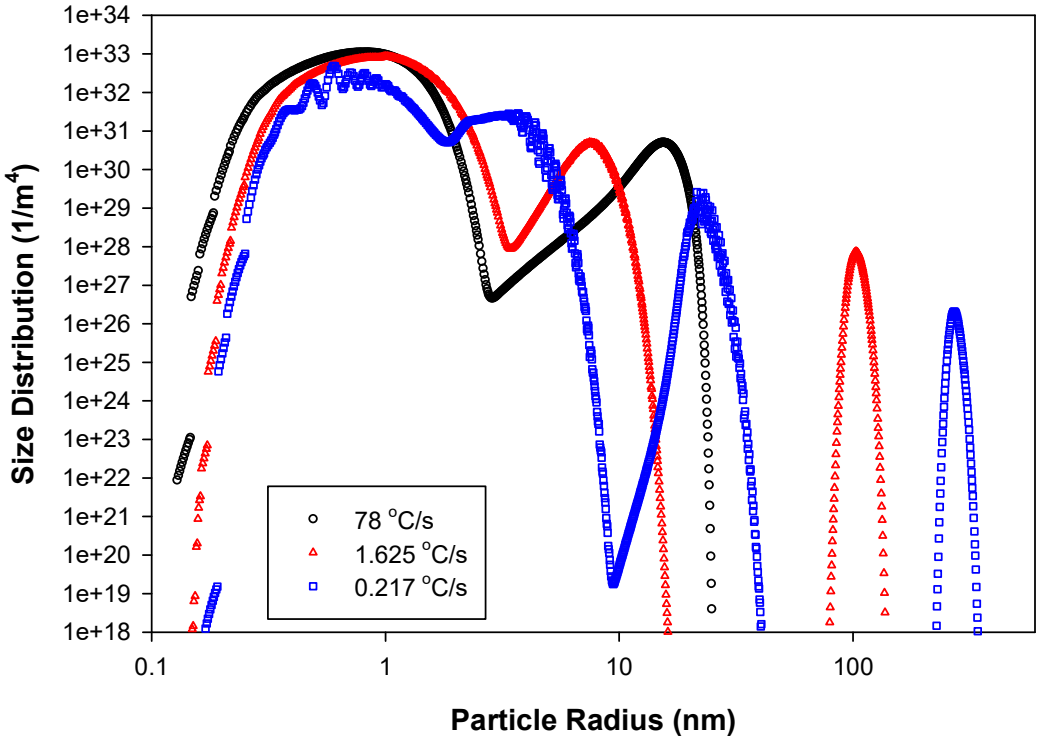

Mean Particle Size

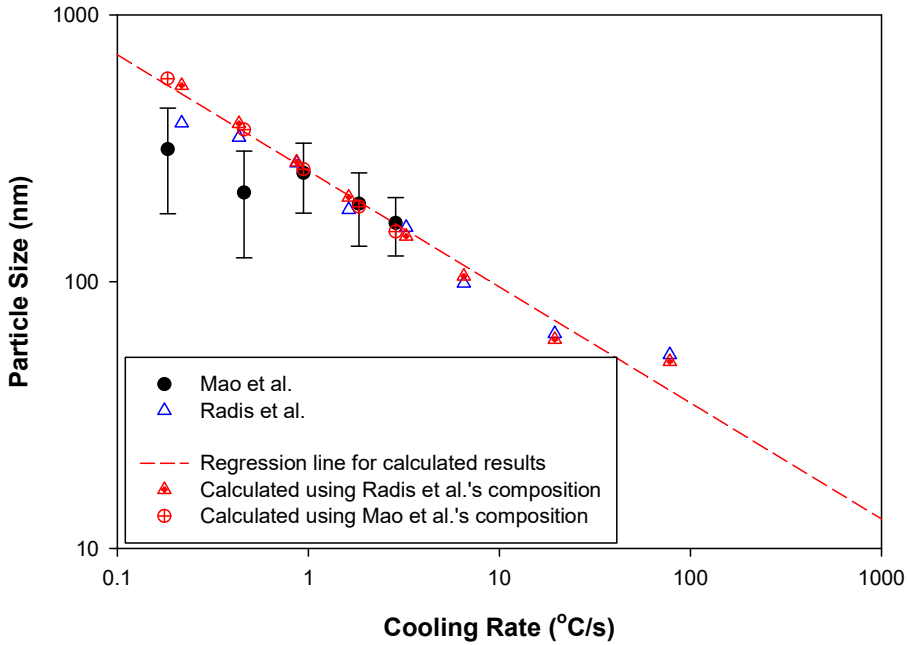

Inconel 718

Co-Precipitation of γ′ and γ″ from FCC (γ) ---

Complex example to try on your own.

γ′ FCC $L1_2$

γ″ BCT DO_{22}

(001) $_{\gamma''}$||{001} $_{\gamma'}$,

[100] $_{\gamma''}$||<100> $_{\gamma}$

Chemical Composition (wt.%)*

Fe	Cr	Nb	Mo	Al	Ti	Ni
18.14	17.9	5.3	2.99	0.5	0.97	Bal.

- γ′ : Sphere + γ″ : Plate
- γ′ misfit strain from database
- γ″* :

Coherency strains ε	$\varepsilon^{T}_{11} = 6.67 \times 10^{-3}$ $\varepsilon^{T}_{33} = 2.86 \times 10^{-2}$
Shear modulus at 1223 K	$\mu = 57.1$ GPa
Poisson's ratio	$\nu = 0.33$

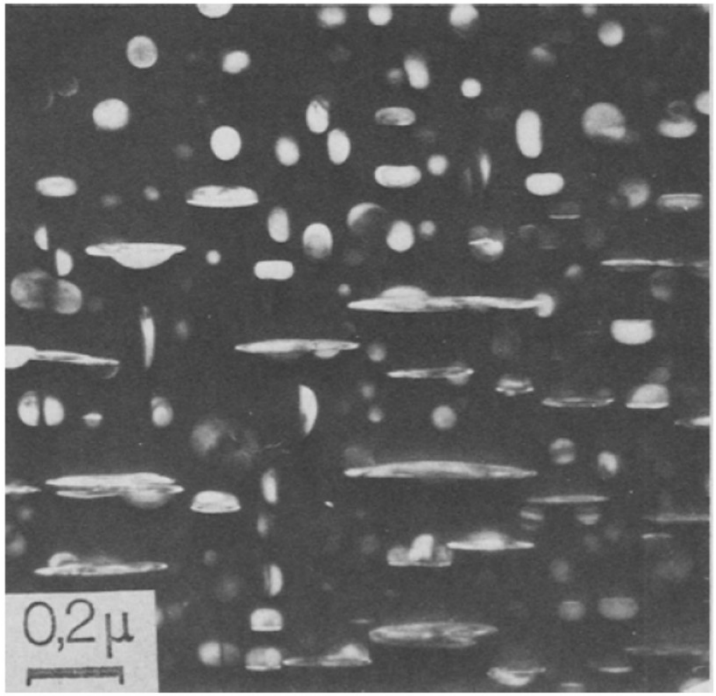

Microstructure of IN718**

* A. Devaux et al. *Mater. Sci. Eng. A* 486(2008)117

** R. Cozar and A. Pineau, *Metall Trans. B* 4(1973)47

Results - IN718 example

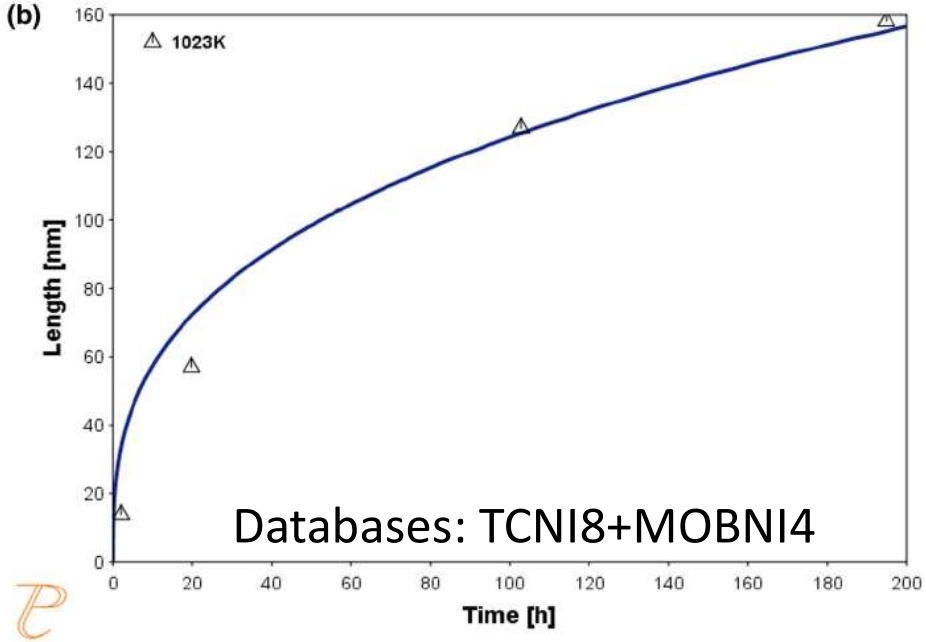

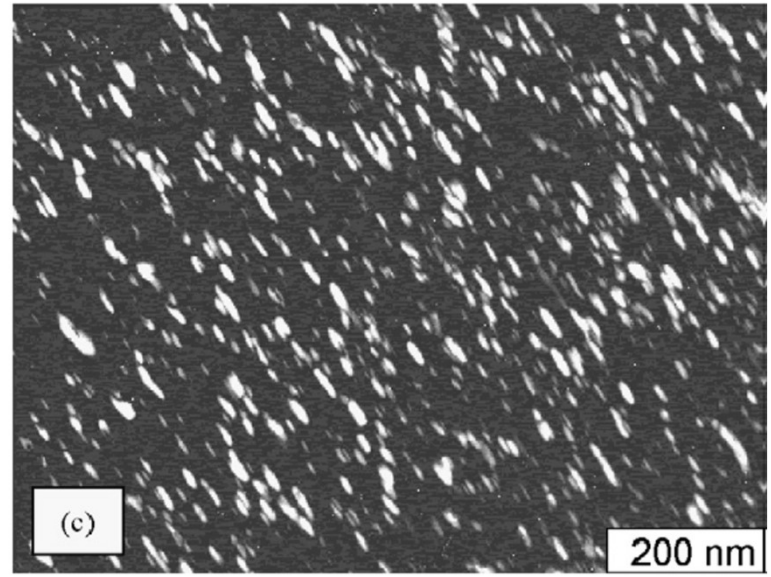

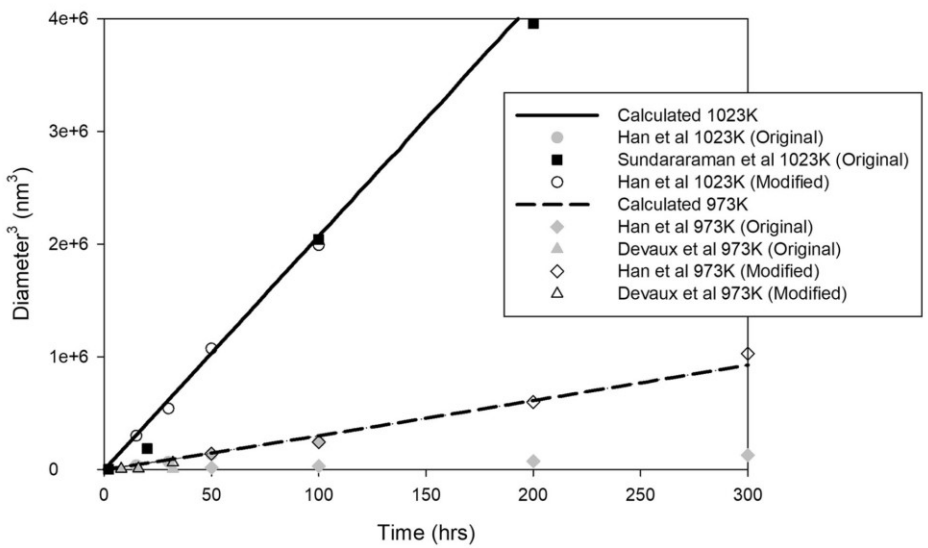

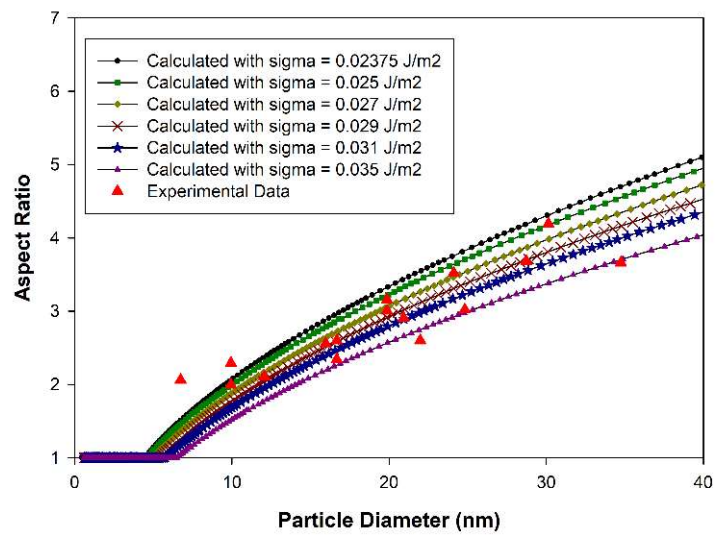

* Experimental Data and Picture from A. Devaux et al. *Mater. Sci. Eng. A* 486(2008)117; M. Sundararaman et al., *Met. Trans. A*, 23(1992)2015

Q & A

Examples

Steel

Multi-precipitates

ELSEVIER

Available online at www.sciencedirect.com

SCIENCE DIRECT®

Acta Materialia 53 (2005) 519–531

Acta MATERIALIA

www.actamat-journals.com

Simulation of the kinetics of precipitation reactions in ferritic steels

A. Schneider *, G. Inden

Department of Materials Technology, Max-Planck-Institut für Eisenforschung GmbH, Max-Planck Straße 1, 40237 Düsseldorf, Germany

Received 15 June 2004; received in revised form 1 October 2004; accepted 4 October 2004
Available online 5 November 2004

Abstract

Computer simulations of diffusion-controlled phase transformations in model alloys of Fe–Cr–C, Fe–Cr–W–C, Fe–Cr–Si–C, and Fe–Cr–Co–V–C are presented. The compositions considered are typical for ferritic steels. The simulations are performed using the software DICTRA and the thermodynamic calculations of phase equilibria are performed using Thermo-Calc. The thermodynamic driving forces and the kinetics of diffusion-controlled precipitation reactions of $M_{23}C_6$, M_7C_3, cementite and Laves-phase $(Fe, Cr)_2W$ are discussed. The simultaneous growth of stable and metastable phases is treated in a multi-cell approach. The results show remarkable effects on the growth kinetics due to the competition during simultaneous growth.

Keywords: Ferritic steels; Phase transformation kinetics; Thermodynamics; Kinetics

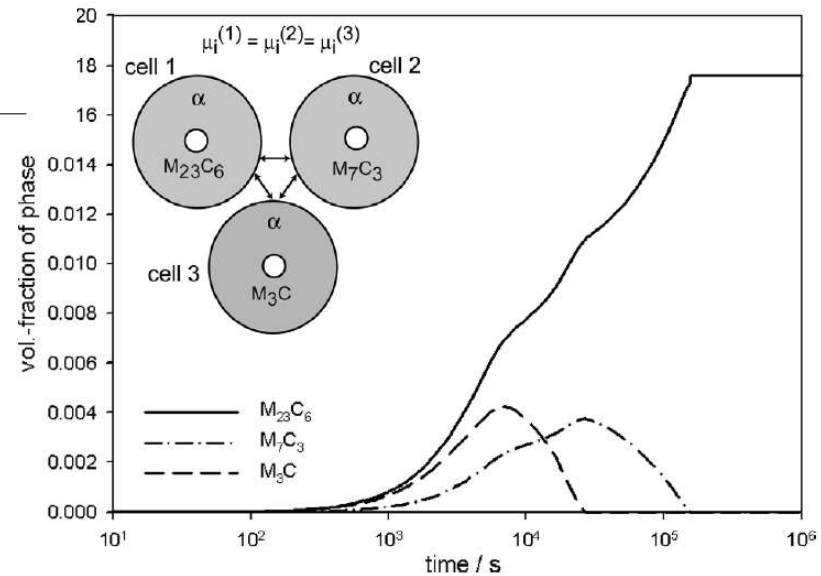

Fig. 6. Three-cell simulation of competitive growth of stable $M_{23}C_6$ and of metastable M_7C_3 and M_3C in Fe–12Cr–0.1C at 1053 were 5 μm and the nucleus sizes were 1 nm in each cell.

Steel Example 1

System	
Database package	TCFE14 + MOBFE8
Elements	Fe, Cr, C
Matrix phase	Bcc_A2
Precipitate phases	$M_{23}C_6$, M_7C_3, Cementite
Conditions	
Composition	Fe – 12 Cr – 0.1 C (wt.%)
Temperature	1053 K
Simulation time	1e6 s
Nucleation properties	Nucleation Site Type: Grain Boundaries
Data Parameters–Interfacial Energies	
Cementite	0.167 J/m^2
$M_{23}C_6$	0.252 J/m^2
M_7C_3	0.282 J/m^2

To include already existing size distributions – see Example 2

Steel Example 1

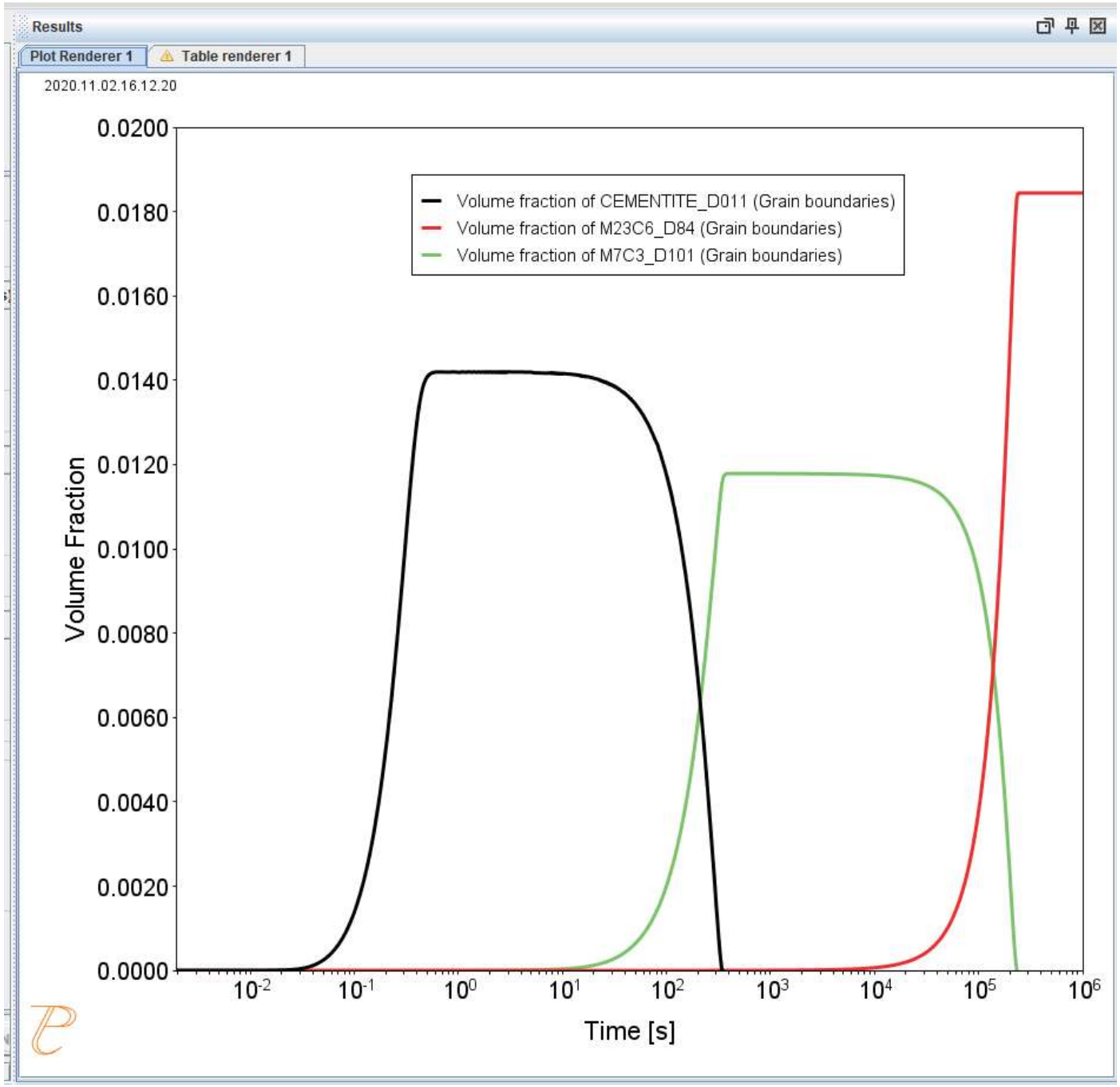

Steel Example 2

Same as Ex 1 but starting from already existing particle distributions of all three carbides, with small mean radius.

LSW
Normal
Log normal
Weibull

Precipitate Phase

Phase:	FCC_L12#2	
Nucleation sites:	Bulk	☑ Calculate f
Interfacial energy:	User-defined	0.023
Growth rate model:	Simplified	
Morphology:	Sphere	
Transformation strain:	Disregard	
Molar volume:	Database	7.0E-6
Phase boundary mobility:	10.0	m^4/Js
Phase energy addition:	0.0	J/mol
Approximate driving force:	☐	
Preexisting size distribution:	☑	Edit particle size distribution

Preexisting Particle Size Distribution

Compositions

Dependent component: Fe Mass percent

Cr 71.4

Size Distribution

Length unit: Meter

Input type: Generate 3D PSD from distribution function

Distribution: LSW Mean radius: 1E-8 Generate

Amount of phase: Volume percent 0.1

Radius [m]	Number Density
1.0E-9	209150.70723283727
1.014E-9	215353.88475874296
1.028E-9	221658.14714236386
1.0420000000000001...	228063.97599748537
1.056E-9	234571.85564586637
1.07E-9	241182.27313133603
1.084E-9	247895.71823396112
1.0980000000000001...	254712.68348428674
1.112E-9	261633.66417764925
1.126E-9	268659.15838856064
1.14E-9	275789.66698516946
1.1540000000000002...	283025.69364379055
1.168E-9	290367.74486351345
1.182E-9	297816.32998087996

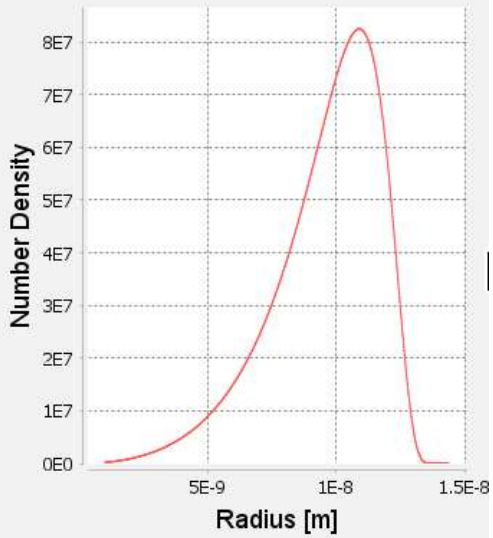

Steel Example 2

Initial Particle Size Distribution	
Phase	CEMENTITE
Initial composition	Cr 71.4 wt.%
Distribution	LSW with mean radius 1.0e-8m
Amount	0.001 (volume fraction)
Initial Particle Size Distribution	
Phase	M23C6
Initial composition	Cr 69.3 wt.%
Distribution	LSW with mean radius 1.0e-8m
Amount	0.0015 (volume fraction)
Initial Particle Size Distribution	
Phase	M7C3
Initial composition	Cr 82.9 wt.%
Distribution	LSW with mean radius 1.0e-8m
Amount	0.0015 (volume fraction)

Steel Example 2

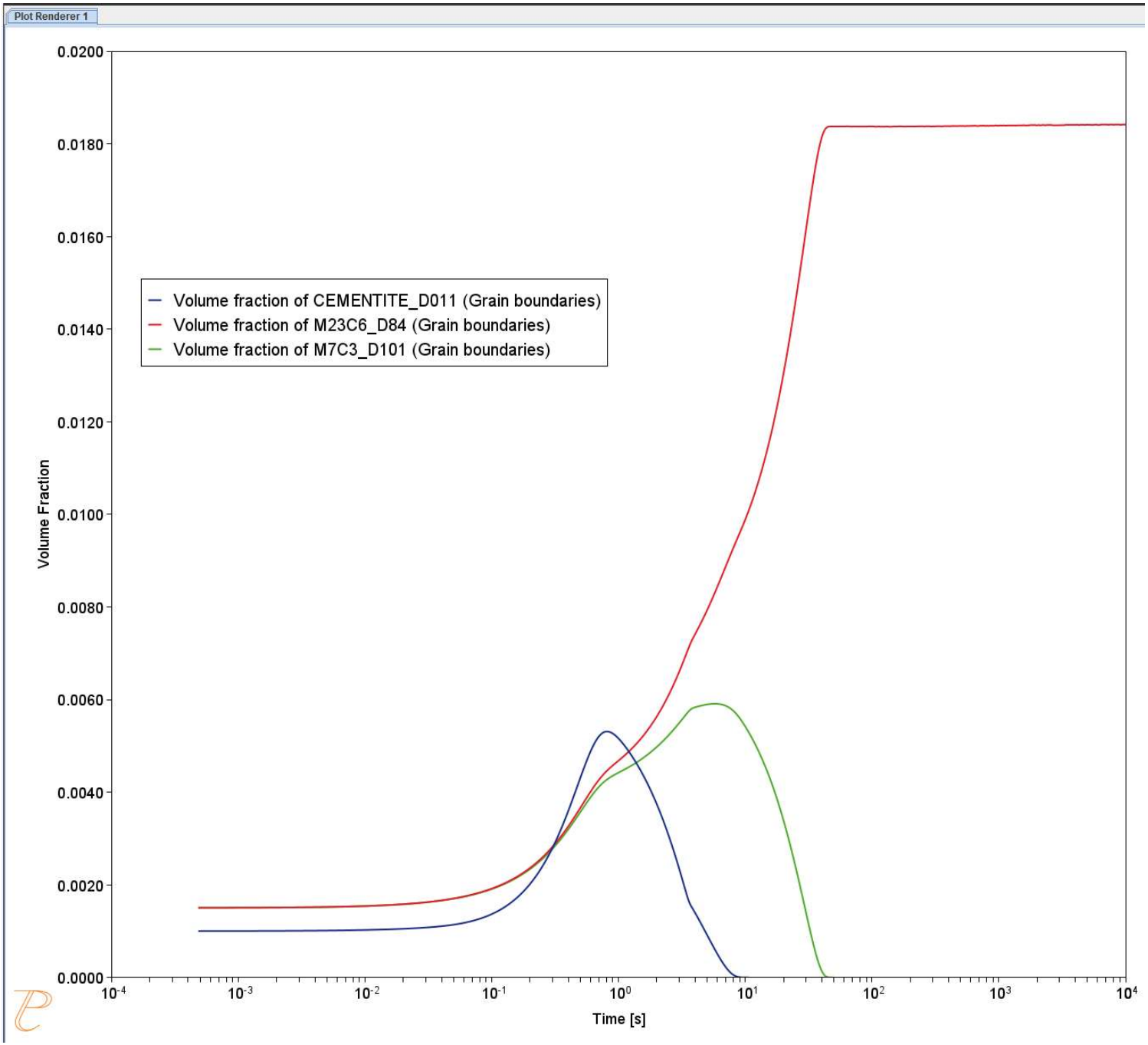

Steel Example 3 – TTP

System	
Database package	TCFE14 + MOBFE8
Elements	Fe,C,Cr,Mn,Ni,Si
Matrix phase	Fcc_A1
Precipitate phase	$M_{23}C_6$

Number of grid points: 15
Maximum number of grid points: 20
Minimum number of grid points: 10

Conditions – TTT diagram	- Phase fraction = 0.001
Composition	Fe-0.068C-20.89Cr-1.61Mn-10.28Ni-0.49Si (wt.%)
Temperature	500 °C, 860 °C, 20 °C
Simulation time	1E7 s
Nucleation properties	Nucleation Site Type: Grain Boundary, Grain size 100 μm

Data Parameters	
Interfacial Energy	Grain Boundary: Calculated

Use the General model

Steel Example 3

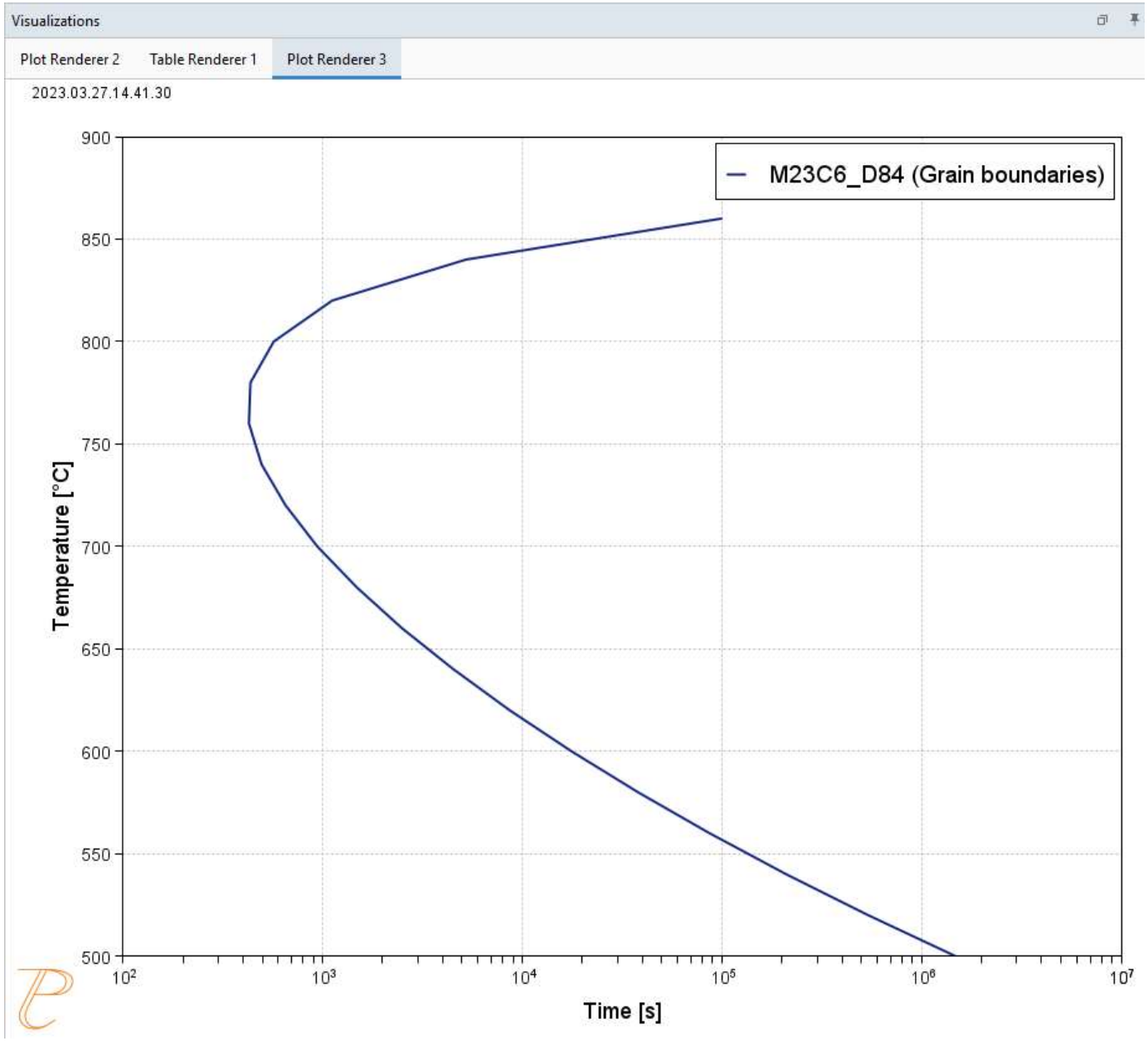

Example

Steel, Para-Equilibrium Models

Para-equilibrium

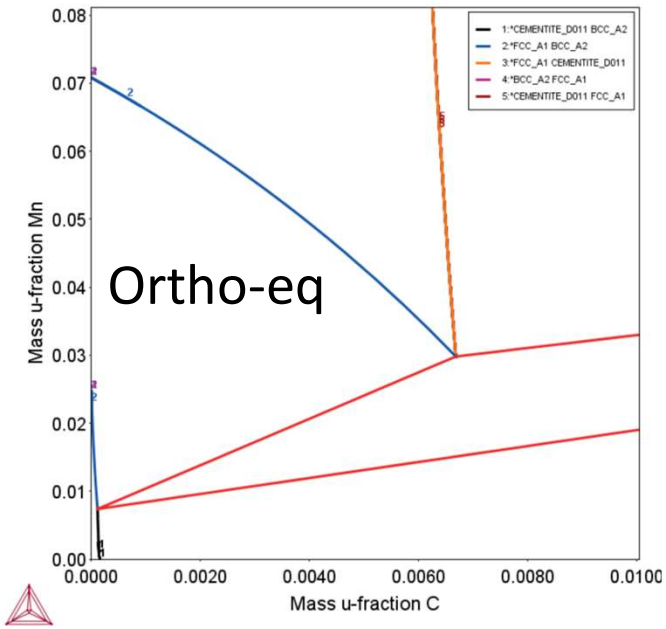

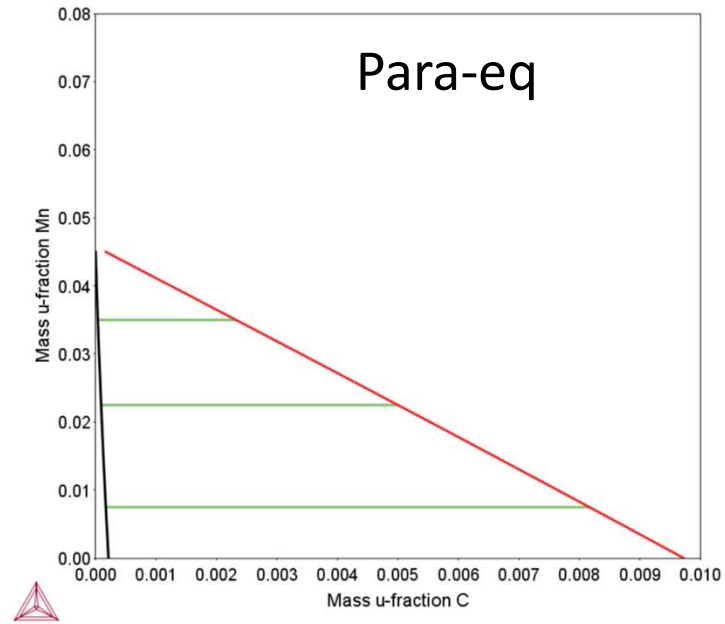

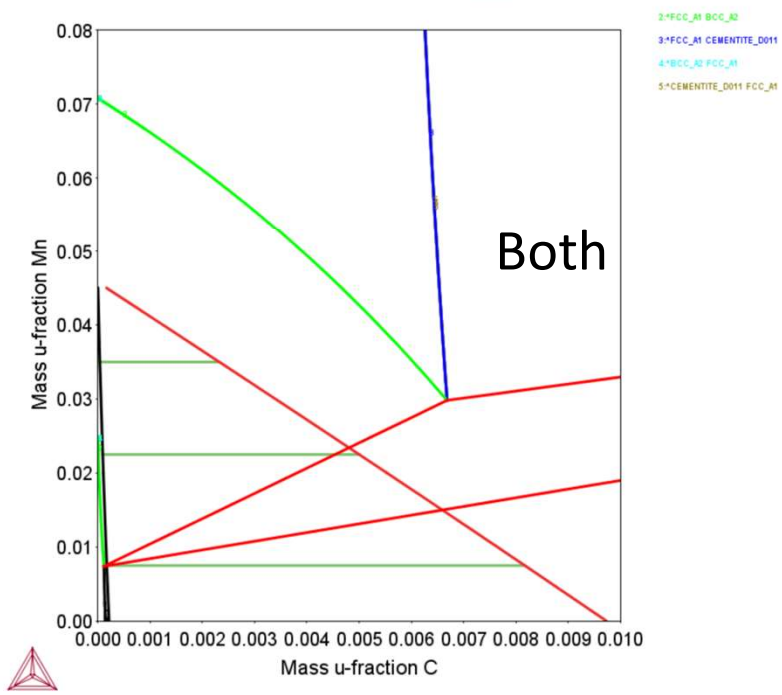

Bcc + Fcc equilibria in Fe – Mn – C

Example: Para-equilibrium or not?

Precipitation of cementite during tempering of martensite in a Fe-Mn-C steel. Consider three different phase interface conditions: the usual ortho-equilibrium condition, para-equilibrium condition, and a smooth transition from para-equilibrium to ortho-equilibrium condition using the recent ***PE Automatic*** growth rate model.

The simulation results can be compared with the experimental data from Miyamoto et al. [2007Miy].

Martensite will be represented by BCC_A2 which requires some rather unusual settings for mobility, grain size and grain shape.

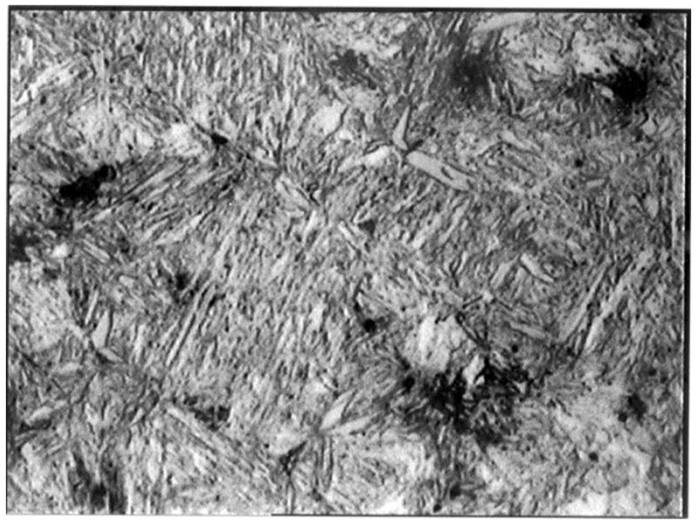

Image from Wikipedia

[2007Miy] G. Miyamoto, J. Oh, K. Hono, T. Furuhara, T. Maki, Effect of partitioning of Mn and Si on the growth kinetics of cementite in tempered Fe–0.6 mass% C martensite. Acta Mater. 55, 5027–5038 (2007).

Example – Para-equilibrium or not?

System	
Database package	FEDEMO + MFEDEMO
Elements	Fe, Mn, C
Matrix phase	BCC_A2
Precipitate phase	Cementite

Conditions	
Composition	Fe- 0.61 C- 1.96 Mn (wt-%)
Temperature	650 °C
Simulation time	1E6 s (5 seconds for PE)
Growth rate models	Simplified / Para-eq / PE Automatic
Nucleation properties	Nucleation Site: Grain boundaries

Data Parameters	
Interfacial Energy	Calculated
Molar Volumes	Database
Grain size / Grain aspect ratio	1E-7 m / 100
Mobility Adjustment factor	0.008
Activation energy	- 70000 J/mol

Example – Para-equilibrium or not?

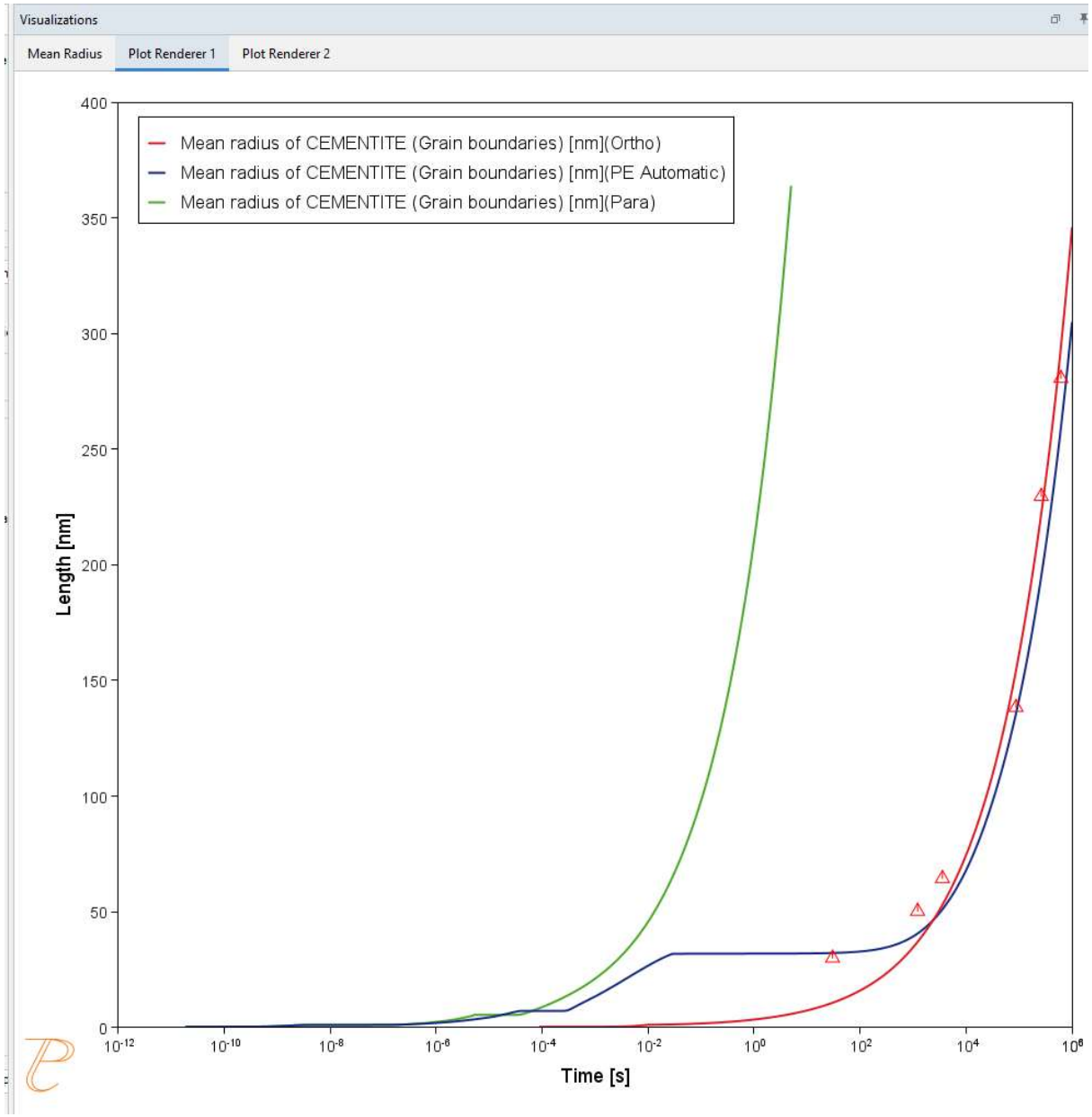

We will send a **course certificate** by email some days after also the AM Online course is finished next week.

Email ake@thermocalc.se if you think we have your name and affiliation incorrect.

Q & A

End of course.